



**UNIVERSIDAD DE INVESTIGACIÓN DE  
TECNOLOGÍA EXPERIMENTAL YACHAY**

**Escuela de Ciencias Biológicas e Ingeniería**

**TÍTULO: REMEDIACIÓN DE LA CONTAMINACIÓN DE  
AGUA POR METALES PESADOS CON EL USO DE  
CELULOSA DE LA BIODIVERSIDAD DE ECUADOR**

Trabajo de integración curricular presentado como requisito para la  
obtención del título de Ingeniero Biomédico

**Autor:**

Figuroa Guayllas Freddy Paúl

**Tutor:**

PhD. Alexis Frank

**Co-Tutor:**

PhD. López Floralba

Urcuquí, Marzo 2020

Urcuquí, 4 de marzo de 2020

**SECRETARÍA GENERAL**  
(Vicerrectorado Académico/Cancillería)  
**ESCUELA DE CIENCIAS BIOLÓGICAS E INGENIERÍA**  
**CARRERA DE BIOMEDICINA**  
**ACTA DE DEFENSA No. UITEY-BIO-2020-00007-AD**

En la ciudad de San Miguel de Urcuquí, Provincia de Imbabura, a los 4 días del mes de marzo de 2020, a las 10:00 horas, en el Aula CHA-02 de la Universidad de Investigación de Tecnología Experimental Yachay y ante el Tribunal Calificador, integrado por los docentes:

<b>Presidente Tribunal de Defensa</b>	<u>Dr. DAHOUMANE , SI AMAR , Ph.D.</u>
<b>Miembro No Tutor</b>	<u>Dr. RAMIREZ CANDO, LENIN JAVIER , Ph.D.</u>
<b>Tutor</b>	<u>Dr. ALEXIS FRANK , Ph.D.</u>

Se presenta el(la) señor(ita) estudiante FIGUEROA GUAYLLAS, FREDDY PAUL, con cédula de identidad No. 0706365137, de la ESCUELA DE CIENCIAS BIOLÓGICAS E INGENIERÍA, de la Carrera de BIOMEDICINA, aprobada por el Consejo de Educación Superior (CES), mediante Resolución RPC-SO-43-No.496-2014, con el objeto de rendir la sustentación de su trabajo de titulación denominado: Remediación de la contaminación de agua por metales pesados con el uso de celulosa de la biodiversidad de Ecuador, previa a la obtención del título de INGENIERO/A BIOMÉDICO/A.

El citado trabajo de titulación, fue debidamente aprobado por el(los) docente(s):

**Tutor** Dr. ALEXIS FRANK , Ph.D.


Y recibió las observaciones de los otros miembros del Tribunal Calificador, las mismas que han sido incorporadas por el(la) estudiante.


Previamente cumplidos los requisitos legales y reglamentarios, el trabajo de titulación fue sustentado por el(la) estudiante y examinado por los miembros del Tribunal Calificador. Escuchada la sustentación del trabajo de titulación, que integró la exposición de el(la) estudiante sobre el contenido de la misma y las preguntas formuladas por los miembros del Tribunal, se califica la sustentación del trabajo de titulación con las siguientes calificaciones:

Tipo	Docente	Calificación
Miembro Tribunal De Defensa	Dr. RAMIREZ CANDO, LENIN JAVIER , Ph.D.	9.6
Presidente Tribunal De Defensa	Dr. DAHOUMANE , SI AMAR , Ph.D.	10.0
Tutor	Dr. ALEXIS FRANK , Ph.D.	10.0

Lo que da un promedio de: 9.9 (Nueve punto Nueve), sobre 10 (diez), equivalente a: **APROBADO**

Para constancia de lo actuado, firman los miembros del Tribunal Calificador, el/la estudiante y el/la secretario ad-hoc.

  
FIGUEROA GUAYLLAS, FREDDY PAUL  
Estudiante

  
Dr. DAHOUMANE , SI AMAR , Ph.D.  
Presidente Tribunal de Defensa

  
Dr. ALEXIS FRANK , Ph.D.  
Tutor



Dr. RAMIREZ-CANDO, LENIN JAVIER , Ph.D.  
Miembro No Tutor

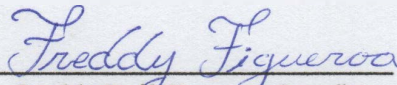


ALARCON FELIX, KARLA ESTEFANIA  
Secretario Ad-hoc

## AUTORÍA

Yo, **Freddy Paúl Figueroa Guayllas**, con cédula de identidad 0706365137, declaro que las ideas, juicios, valoraciones, interpretaciones, consultas bibliográficas, definiciones y conceptualizaciones expuestas en el presente trabajo; así como, los procedimientos y herramientas utilizadas en la investigación, son de absoluta responsabilidad de el/la autor(a) del trabajo de integración curricular. Así mismo, me acojo a los reglamentos internos de la Universidad de Investigación de Tecnología Experimental Yachay.

Urcuquí, marzo 2020.

  
Freddy Paúl Figueroa Guayllas  
CI: 0706365137

## AUTORIZACIÓN DE PUBLICACIÓN

Yo, **Freddy Paúl Figueroa Guayllas**, con cédula de identidad 0706365137, cedo a la Universidad de Tecnología Experimental Yachay, los derechos de publicación de la presente obra, sin que deba haber un reconocimiento económico por este concepto. Declaro además que el texto del presente trabajo de titulación no podrá ser cedido a ninguna empresa editorial para su publicación u otros fines, sin contar previamente con la autorización escrita de la Universidad.

Asimismo, autorizo a la Universidad que realice la digitalización y publicación de este trabajo de integración curricular en el repositorio virtual, de conformidad a lo dispuesto en el Art. 144 de la Ley Orgánica de Educación Superior

Urcuquí, marzo 2020.

  
Freddy Paúl Figueroa Guayllas  
CI: 0706365137

## **Dedication**

This thesis is dedicated:

To my parents Fredy Figueroa and Enny Guayllas who have allowed me to study in this prestigious University, Yachay Tech, and supported me during my stance in this institution and encouraged me during my studies. Thanks for inspiring me to be a professional, and having a good career.

To my siblings, Saúl and Marilyn Figueroa, for their unconditional love and support, for helping me during my last steps in University. Also, to my grandmothers, Leticia Castillo and Julia Samaniego, for their advices, prayers, and good wishes to me. Their words of encouragement made me a better person.

Finally, to all the people involved in the development of this thesis including my tutor, Dr. Frank Alexis, co-tutor, Ph.D. Floralba López, and Ph.D. Thibault Terencio, as well as my partners, Fernanda Romero, Isaac Bravo, Bryan Aldaz, Cristhian Preciado and Luis Sarmiento for supporting me in difficult moments during my life in the University.

## **Acknowledgement**

I would like to thank the School of Biological Sciences and School of Chemical Sciences for give me the opportunity and the facilities to perform my experiments in the laboratories. Also, I appreciate the collaboration from Mechanical Engineering Faculty, ESPE, in particular PhD. Alexis Debut for helping with the characterization data showed in the present thesis project.

I would like to thank my supervisors PhD. Frank Alexis and PhD. Floralba Lopez for guiding me during the performance of the thesis project. Also, I would like to thanks PhD. Thibault Terencio for being a good mentor in the use of UV-Vis-NIR machine and for spending his time to teach me how to use this equipment.

## RESUMEN

Los iones de metales pesados son sustancias tóxicas comúnmente encontradas, son liberados en el agua por diversas fuentes antropogénicas. Varios materiales orgánicos e inorgánicos han sido usados para la remediación de los contaminantes de agua. No obstante, existe una evidente atracción en el desarrollo de materiales sostenibles y amigables con el ambiente. Celulosa novedosa no modificada extraída de fuentes naturales únicas del Ecuador emerge como un adsorbente eficiente de iones de metales pesados presentados en agua contaminada (e.g.  $\text{Cu}^{2+}$ ,  $\text{Ag}^+$ ). La celulosa comercialmente disponible (e.g. micro-cristales de celulosa) fue usada como un control para probar la capacidad de adsorción de la celulosa con los cationes previamente mencionados. Ensayos de espectroscopia UV-Vis-NIR demostraron que la celulosa no tratada adsorbió satisfactoriamente los iones de metales pesados, tales como los iones de cobre, describiendo una notable disminución en el pico característico de  $\text{Cu}^{2+}$  en muestras que contienen celulosa. Los resultados sugieren que los materiales basados en celulosa pueden ser una solución potencial, amigable con el medio ambiente y menos costosa para la descontaminación de los contaminantes del agua, específicamente los iones de metales pesados.

**Palabras Clave:** Celulosa, iones de metales pesados, contaminación del agua, biodiversidad



## ABSTRACT

Heavy metal ions are commonly encountered toxic substances released into the water from diverse anthropogenic sources. Numerous organic and inorganic materials have been used for remediation of water pollutants. However, there is an evident attraction in sustainable and ecofriendly materials development. Novel unmodified cellulose extracted from unique natural sources in Ecuador has emerged as an effective adsorbent of heavy metal ions presented in water pollution (e.g.  $\text{Cu}^{2+}$ ,  $\text{Ag}^+$ ). Commercially available cellulose (e.g. cellulose microcrystals) was used as a control to test cellulose adsorption capacity of previously mentioned cations. UV-Vis-NIR spectroscopy assays proved that non-treated cellulose successfully adsorbed heavy metal ions, such as copper ions, depicting a notable diminution in the characteristic peak of  $\text{Cu}^{2+}$  in samples containing cellulose. Results suggested that cellulose-based materials can be a potential, environmental friendly, less expensive solution for decontamination of water pollutants, specifically heavy metal ions.

**Keywords:** Cellulose, heavy metal ions, water pollution, biodiversity.

## Index

<b>1. Introduction: Theoretical Framework</b> .....	1
<b>1.1. Heavy metals</b> .....	1
<b>1.2. Cellulose</b> .....	2
<b>1.3. Cellulose applications for remediation of polluted water</b> .....	3
<b>1.4. Current innovation in remediation of heavy metal water pollution</b> .....	5
<b>2. Problem Statement</b> .....	7
<b>2.1. Heavy metal water pollution in Ecuador</b> .....	8
<b>3. Hypothesis, General and Specific Objectives</b> .....	10
<b>3.1. Hypothesis</b> .....	10
<b>3.2. General Objective</b> .....	10
<b>3.3. Specific Objectives</b> .....	10
<b>4. Methodology</b> .....	11
<b>4.1. Materials</b> .....	11
<b>4.2. Cellulose samples preparation</b> .....	11
<b>4.3. Cellulose samples characterization</b> .....	11
<b>4.4. Aqueous solutions of heavy metals</b> .....	13
<b>4.5. Cellulose-treated solutions</b> .....	13
<b>4.6. UV-Vis-NIR assays</b> .....	14
<b>4.7. Statistical analysis</b> .....	15
<b>5. Results</b> .....	16
<b>5.1. Characterization of commercially available cellulose (i.e. Cellulose Micro-Crystals (CMC)) as a control</b> .....	16
<b>5.2. Characterization of cellulose samples extracted from natural sources</b> .....	18
<b>5.3. UV-Vis-NIR assays on standard heavy metal solutions</b> .....	21
<b>5.4. Percentages of removal of copper in cellulose-copper adsorption assays</b> .....	24
<b>5.5. Statistical analysis</b> .....	26
<b>5.6. Nanoparticles formation in cellulose-silver suspensions</b> .....	33
<b>5.7. Samples surface properties</b> .....	34
<b>6. Discussion</b> .....	35
<b>7. Conclusion</b> .....	37
<b>8. Recommendations</b> .....	38
References.....	40
Annex A.....	44
Annex B.....	47

## List of Schemes

Scheme 1	Flow-chart of the objectives of this research.....	10
Scheme 2	Flow-chart of the UV-NIR procedure for cellulose-treated solutions.....	15

## List of Tables

Table 1	Toxicity issues and Maximum Contaminants Levels (MCL) standards of hazardous heavy metals.....	2
Table 2	Adsorption capacities of modified cellulose-based materials for Cu(II) ions.....	3
Table 3	Potential nanomaterials screened for remediation of heavy metal water pollution	6
Table 4	Percentage of Ecuadorian Population covered with basic services.....	9
Table 5	Concentrations of heavy metal solutions.....	13
Table 6	ANOVA of the absolute concentration values of copper-cellulose suspensions (0.004 M).....	26
Table 7	ANOVA of the absolute concentration values of copper-cellulose suspensions (0.02 M).....	28
Table 8	ANOVA of the absolute concentration values of copper-cellulose suspensions (0.04 M).....	30
Table 9	Statistical analyses (mean, standard deviation, coefficient of variation (CV) and statistical significance) of copper remaining percentages for the different cellulose-copper suspensions using 1 mg/mL of cellulose samples.....	32
Table 10	Statistical analyses (mean, standard deviation, coefficient of variation (CV) and statistical significance) of copper remaining percentages for the different cellulose-copper suspensions using 10 mg/mL of cellulose samples.....	33
Table 11	Specific Surface Area (SSA) and Pore Volume (PV) of cellulose samples.....	34
Table 12	Maximum values of absorbance of cellulose-copper suspensions.....	44
Table 13	Copper remaining percentages in cellulose-copper suspensions.....	45
Table 14	Values of absolute concentration in cellulose-copper suspensions.....	46

## List of Graphs

Figure 1	FTIR spectrum of control sample: Cellulose microcrystals.....	16
Figure 2	XRD pattern of control sample: Cellulose microcrystals.....	17
Figure 3	SEM micrographs of the control sample: Cellulose microcrystals.....	17
Figure 4	FTIR spectra of F20, F25, F28 and T1 cellulose samples .....	18
Figure 5	XRD patterns of F20, F25, F28 and T1 cellulose samples.....	19
Figure 6	SEM micrographs of F20 cellulose sample.....	20
Figure 7	SEM micrographs of F25 cellulose sample.....	20
Figure 8	SEM micrographs of F28 cellulose sample .....	21
Figure 9	SEM micrographs of T1 cellulose sample.....	21
Figure 10	Absorption spectra of copper aqueous solutions .....	22
Figure 11	Calibration curve of copper standard solutions (max wavelength: 813 nm).....	22
Figure 12	Absorption spectra of silver aqueous solutions.....	23
Figure 13	Calibration curve of silver standard solutions (max wavelength: 302 nm).....	23
Figure 14	Percentages of removal of copper in F20-copper suspensions.....	24
Figure 15	Percentages of removal of copper in F28-copper suspensions.....	24
Figure 16	Percentages of removal of copper in F25-copper suspensions.....	25
Figure 17	Percentages of removal of copper in T1-copper suspensions.....	25
Figure 18	Validation graphs of (A) square root of the standardized residuals and the fitted values, (B) the standardized residuals and the theoretical quantiles, and (C) measured vs predicted values of ANOVA of cellulose-copper suspensions (0.004 M).....	27
Figure 19	Significance differences among the means of first order effects. (A) Cellulose samples, and (B) amount of cellulose used in cellulose-copper suspensions (0.004 M).....	28
Figure 20	Validation graphs of (A) square root of the standardized residuals and the fitted values, (B) the standardized residuals and the theoretical quantiles, and (C) measured vs predicted values of ANOVA of cellulose-copper suspensions (0.02 M).....	29
Figure 21	Significance differences among the means of first order effects. (A) Cellulose samples, and (B) amount of cellulose used in cellulose-copper suspensions (0.02 M).....	30
Figure 22	Validation graphs of (A) square root of the standardized residuals and the fitted values, (B) the standardized residuals and the theoretical quantiles, and (C) measured vs predicted values of ANOVA of cellulose-copper suspensions (0.04 M).....	31
Figure 23	Significance differences among the means of first order effects. (A) Cellulose samples, and (B) amount of cellulose used in cellulose-copper suspensions (0.04 M).....	32
Figure 24	Absorption spectra of T1-silver suspensions.....	34
Figure 25	Correlation between PV and SSA.....	35

## **1. Theoretical framework**

### **1.1. Heavy metals**

Heavy metals as a collective term can be defined as any metallic element that has a relatively high density, depicting an atomic density greater than  $4 \text{ g/cm}^3$ , or at least 5 times greater than that of water (Ahmad et al., 2020; Tchounwou et al., 2012). Nevertheless, its definition concerns chemical properties rather than density. Heavy metals include copper (Cu), cadmium (Cd), Zinc (Zn), lead (Pb), mercury (Hg), arsenic (As), silver (Ag), chromium (Cr), Iron (Fe) and the platinum (Pt) group elements (Duruibe et al., 2007). These commonly encountered toxic molecules are released into water from diverse anthropogenic sources, including human settlements, industrial and mining activities, and agricultural sources (Duruibe et al., 2007; Inyinbor Adejumo et al., 2018; Tchounwou et al., 2012; Tian et al., 2011). Additionally, they can enter a water supply by industrial and consumer waste, or even from acidic rains releasing heavy metals into streams, lakes, rivers and groundwater (Abiaziem et al., 2019; Verma & Dwivedi, 2013).

Heavy metals are dangerous to health and to the environment because they tend to bioaccumulate, which means the over-time concentration increase of a chemical in a biological organism. Heavy metal toxicity can result in damaged or reduced mental and central nervous functions (Verma & Dwivedi, 2013). Therefore, metallic elements listed in Table 1 are considered systemic toxicants known to induce multiple organ damage affecting lungs, kidneys and liver, even at lower levels of exposure than the maximum contaminant level (MCL) standards established for drinking water (Abiaziem et al., 2019; INEN, 2014; Tchounwou et al., 2012). Long-term exposure to heavy metals may result in a slowly progressing physical, muscular and neurological degenerative processes, and may eventually cause cancer (Jaishankar et al., 2014).

**Table 1. Toxicity issues and Maximum Contaminants Level (MCL) standards of hazardous heavy metals (Barakat, 2011; INEN, 2014).**

Heavy metal	Toxicities	MCL (mg/L)
Arsenic	Skin manifestations, visceral cancers, vascular disease	0.01
Cadmium	Kidney damage, renal disorder, human carcinogen	0.003
Chromium	Headache, diarrhea, nausea, vomiting carcinogenic	0.05
Copper	Liver damage, Wilson disease, insomnia	2.0
Nickel	Dermatitis, nausea, chronic asthma, coughing, human carcinogen	0.07
Zinc	Depression, lethargy, neurological signs and increased thirst	0.80
Lead	Damage the fetal brain, diseases of the kidneys, circulatory and nervous systems	0.01
Mercury	Rheumatoid arthritis, diseases of the kidneys, circulatory and nervous systems	0.006

## 1.2. Cellulose

Cellulose is the most abundant biopolymer that can be obtained from a variety of biodiverse natural sources (Anwar et al., 2015; Bethke et al., 2018; Mihranyan, 2010; Morán et al., 2008). This natural polymer is composed by repeating monosaccharides formed of 2-D-glucopyranose units linked by  $\beta$ -1,4-glycosidic bonds (Guerra et al., 2018; Nabili et al., 2014; Thakur & Thakur, 2014). Its surface structure possesses abundant hydroxyl groups, therefore it can be easily functionalized by diverse chemical methods in order to enhance its physicochemical properties (Phanthong et al., 2018; Wang et al., 2018). Cellulose has been of particular interest due to its huge availability worldwide, low cost, flexibility, easy processing, nontoxic, biodegradable and unique physicochemical properties (Thakur & Thakur, 2014). Many studies have focused on cellulose-based materials renewability, versatility and functionality for many remediation applications, such as removal of heavy metal ions in water (Bethke et al., 2018; Carpenter et al., 2015; George & Sabapathi, 2015; Ma et al., 2011; O'Connell et al., 2008; Wan Ngah & Hanafiah, 2008).

Cellulose is a water-insoluble material and the major component of the cell wall of numerous types of algae and plants (Brigham, 2018; Dhyani & Bhaskar, 2019). Recently, many sources of cellulose are being studied, including plants, algae, microorganisms and marine fauna (Lavanya, Kulkarni, & Dixit, 2011). Plants have emerged as the main source for cellulose extraction besides commonly reported sources, namely wood pulp

and cotton linters, due to their abundance, variety and financial viability. Furthermore, agricultural activity provides sustainable waste, such as sugarcane bagasse, fruits, seeds, grasses or rice straws, which are ideal sources for the extraction of cellulose. Many bacteria through internal biochemical processes can produce this natural polymer. In addition, bacterial cellulose presents several advantages over plant-derived cellulose, including unique nanostructure, purity, higher-dimensional stability, greater mechanical strength and polymerization. Additionally, the marine invertebrate Tunicates are well-known for assembling cellulose. These sea animals use cellulose as a skeletal structure in their leathery mantle tissues, which is produced by enzyme complexes found in the membrane of the tunicate epidermis (George & Sabapathi, 2015).

### 1.3. Cellulose applications for remediation of polluted water

Currently, the scientific community and academia have focused on remediation application by using novel, economical viable and environmentally friendly solutions. In fact, there is a special attention in biopolymers such as cellulose. Numerous studies have demonstrated that cellulose is a suitable natural polymer for the development of remediation technologies, mainly used for the decontamination of polluted water (Varghese et al., 2018). Moreover, cellulose remediation capacities can be significantly enhanced by chemical modifications on cellulose surface. Indeed, functionalized cellulose have shown excellent results for copper (II) removal from polluted water, as illustrated in Table 2 (Bethke et al., 2018).

**Table 2. Adsorption capacities of modified cellulose-based materials for Cu(II) ions (Bethke et al., 2018).**

Adsorbent	Modification (binding functional group)	Capacity [mmol/g]
Cellulose	TEMPO oxidation, PEI grafting (carboxyl and amine)	0.82
Kapok	Coated with poly-acrylonitrile	1.42
Wood pulp	Glycidyl methacrylate and imidazole	1.75
Cellulose sugarcane bagasse	1,3-Diisopropyl-carbodiimide (amine)	1.79
Cellulose Paper	PEI-crosslinked	6.84

Besides the usage of modified cellulosic materials for the efficient adsorption of pollutants, cellulose-based nano- and micro-scale materials can be engineered and explored for the fabrication of filtration membranes for water treatment (Carpenter et al., 2015). S. Wang et al., 2013 indicated that advancing productive microfiltration membranes can be reached by the integration of ultrafine cellulose nanofibers onto a platform based on a nanoscale layer polyacrylonitrile (PAN) deposited on a microscale polyethylene terephthalate (PET) film. They demonstrated that crucial parameters for cellulose water remediation capacities are surface area and porosity degree since larger surface area and wider pores can improve bacterial retention, and the adsorption of heavy metals and other common contaminants in water. Thus, these membranes are interesting as they can remove toxic pollutants turning into a promising device for use in drinking water decontamination.

Many other synthetic polymers have been combined with cellulose in order to test and evaluate their remediation capacities. As detailed by Guclu et al., 2003, cellulose graft copolymers can lead to applications for the removal of heavy metal water pollutants. They hypothesized that the ion-exchange property of the biomaterial is a critical factor that influences the capturing capacities of Pb(II), Cu(II), and Cd(II) particles. They utilized many copolymers including cellulose-g-polyacrylic corrosive (cellulose-g-pAA) with various grafting rates, cellulose-g-p(AA–NMBA) arranged by grafting of acrylic acid (AA) onto cellulose within the presence of crosslinking operator of N, N-methylene bisacrylamide (NMBA), cellulose-g-p(AA–AASO<sub>3</sub>H) arranged by grafting of a monomer mixture of AA and 2-acrylamido-2-methyl propane sulfonic acid (AASO<sub>3</sub>H), and cellulose-g-pAASO<sub>3</sub>H acquired by grafting of AASO<sub>3</sub>H onto cellulose. Results demonstrated that every cellulose copolymer tested displayed a selective removal for specific heavy metal particles. Moreover, Waly et al., 1998 showed that, among numerous copolymers studied (e.g. glycidyl methacrylate, dimethyl aminoethyl methacrylate, and polyacrylic acid (pAA)), pAA-cotton cellulose-based copolymer was the most dynamic/active biomaterial regarding the removal of metallic particles, specifically Cu(II) and Co(II), and presented great effectiveness for capturing basic dyes.



Although heavy metal removal using cellulosic materials is the most studied research topic currently, cellulose can be further investigated and applied for other water remediation applications. For instance, Tursi et al., 2018, demonstrated that surface-hydrophobic cellulose strands extracted from Spanish Broom (SB) are an appropriate material for the rapid and considerable adsorption of hydrophobic organic compounds (HOCs) present in water contamination. In particular, the surface of the SB cellulose strands can be altered by conventional chemical nebulization utilizing 4,4'-diphenylmethane diisocyanate, therefore the hydrophilic surface properties of the polymer are removed. Once the functionalization of the cellulose is confirmed by XPS and ATR-FTIR spectroscopies, researchers performed batch analyzes in order to test the adsorption kinetics and limit of the strands to remediate contaminated water with fuel petroleum. The outcomes uncovered in this investigation effectively demonstrate that this functionalized SB cellulose fiber can adsorb oil hydrocarbons with an efficiency greater than 90% in a short period of time (min), which makes this biomaterial a novel green innovation for the remediation of contaminated water.

#### **1.4. Current innovation in remediation of heavy metal water pollution**

Recent advances in nanotechnology allow the manufacturing of porous nanomaterials including metal oxide nanoparticles, carbon nanomaterials and nanocomposites as adsorbents. Adsorption is one of the most utilized methods for the remediation of water pollution due to its simplicity, flexibility and cost-effectiveness. Nanomaterials used as adsorbents for heavy metal removal from polluted water should be inert and exhibit nontoxic properties, high adsorptive capacities and selectivity, and reversible adsorption process (Lee, Abbas, Zaini, & Tang, 2019).

**Table 3. Potential nanomaterials screened for the remediation of heavy metal water pollution (Lee et al., 2019).**

Nanomaterial	Synthesis method	Example	Advantage	Disadvantage
Metal oxide nanoparticle	Chemical coprecipitation Hydrothermal reaction	Ferric oxides (hematite, maghemite, and magnetite) Manganese oxides Aluminum oxide Titanium oxides Magnesium oxides	Large surface area High surface activities Minimal environmental impact Low solubility No secondary pollution	Very difficult to be separated from wastewater Excessive pressure drop in continuous systems
Carbon nanomaterial	Chemical vapor deposition Hummers method	Carbon nanotubes Carbon nanofibers Graphite oxides	Nontoxicity High specific surface area Good mechanical and thermal properties	Difficult to be separated from wastewater
Nanocomposite	Chemical coprecipitation Ion exchange	Polymer-supported nanocomposites Nano-MnO <sub>2</sub> -biochar	Chemically stable Presence of various reactive chemical groups	Required more processes/procedures during synthesis

Table 3 presents relevant data concerning the different porous nanomaterials that can be used for the depollution of water including their synthesis process, examples of products, advantages and disadvantages. Data showed that physicochemical properties of materials (porosity and pore volume, morphology and surface area) are critical factors affecting the adsorption capacities.

Recently, phycoremediation has emerged as a potential, eco-friendly tool for the removal of heavy metal in polluted water. The algal-based heavy metal remediation works on the principle of biosorption either by passive sorption of pollutant independently of metabolic processes or active sorption of pollutants correlated to metabolic pathways.

Due to their physicochemical properties, such as large surface/volume ratios and the presence of high-affinity metal-binding groups on their surfaces, algal species are considered a promising, environmentally friendly and sustainable solution for the decontamination of heavy metal water pollution. Nevertheless, there are several environmental factors such as pH, temperature, and contact time, that affect the biosorption capacity (Ahmad et al., 2020).

Porous nanomaterials are examples of inorganic materials useful for remediation of heavy metal water pollution. On the other hand, algae species are examples of organic/natural materials that can be utilized for the decontamination of polluted water.

## **2. Problem statement**

Water pollution is defined as the contamination of water by inorganic or organic foreign matter that affects negatively the water quality. The term involves pollution in liquid forms, and therefore occurs in the oceans, lakes, rivers, streams, underground water and bays. It is caused by the release of toxic metallic substances, pathogenic germs, water-soluble molecules, radioactive elements, etc. that may accumulate in the water, thus interfering with normal conditions of aquatic environments (Verma & Dwivedi, 2013). The increasing rates of urbanization and industrialization, and agricultural activities along with the inadequate management of wastewater means the drinking-water of hundreds of millions of people is dangerously contaminated or chemically polluted (Inyinbor Adejumo et al., 2018). According to the UN Environment Programme (UNEP), 2 million tons of sewage, industrial and agricultural waste are released into aquatic environments every day around the world; at the same time, one child under the age of five dies every 20 seconds from water-related diseases.

In least developed countries, 22% of health care facilities have no water service, 21% no sanitation service, and 22% no waste management service, facilitating the transmission of diseases such as cholera, diarrhea, dysentery, hepatitis A, typhoid, and polio due to contaminated water and poor sanitation (WHO, 2001). Indeed, contaminated drinking water is estimated to cause 485000 diarrheal deaths every year. According to World Health Organization (WHO), 785 million people lack even a basic drinking-water service, including

144 million people who are dependent on surface water (<https://www.who.int/news-room/fact-sheets/detail/drinking-water>).

WHO compiled a list of the 10 major chemicals of concern, which includes many heavy metals such as mercury, lead, cadmium and arsenic. Heavy metal pollution can arise from many sources but often arises from metal purification processes. For instance, 62000 tons of arsenic are emitted annually from smelting. Arsenic poisoning of groundwater and soils related to mining activities are found in Thailand, Ghana, Zimbabwe, South Africa, England, Greece, Canada, the United States and Latin America countries (Bissen et al., 2003; McClintock et al., 2012). In fact, more than 100 million people are exposed to elevated levels of arsenic, mainly via drinking water, but also via industrial emissions (WHO, 2011).

### **2.1. Heavy metal water pollution in Ecuador**

The expanding rates of illegal and artisanal mining activities in Ecuador have triggered an increase in heavy metal pollution (*i.e.* Cu(II), Pb(II), Cd(II), Hg(II)), thus affecting many water sources located in the surroundings of mining human settlements (González et al., 2018; Oviedo-Anchundia et al., 2017; Unemi, 2016). These metal contaminants are daily released into Ecuadorian rivers generally in water-insoluble forms resulting in an accumulation of metals that could lead to a decrease in aquatic biodiversity (Tarraswahlberg et al., 2001). For instance, gold mining in Portovelo and Zaruma, cities of Ecuador, is producing toxic mercury residuals, cyanide-rich tailings and liquid effluents that are dispensed into local rivers. This fact has contributed to elevated levels of mercury in fish and humans in the region. In addition, waterways where these contaminant materials are discharged are connected to agricultural and aquaculture sectors (Velásquez et al., 2010). Another city affected by mining activity is Ponce Enriquez, where many heavy metal pollutants from mining have accumulated in river ecosystems and agricultural areas. Further downstream, the large shrimp farming industry is impacted too as contaminants are in high concentrations; this has affected estuarine regions and mangrove areas where mercury methylation can occur (Enr et al., 2019). Similarly, many rivers in north Ecuador, in Esmeraldas Province, have been contaminated with several heavy metals due to illegal gold mining and poor management of toxic wastes. Most of

the rivers analyzed by Rebolledo et al presented alarming concentrations of heavy metals (Rebolledo & Jiménez, 2012).

**Table 4. Percentage of Ecuadorian Population covered with basic services (Harari & Harari, 2006).**

Region	Public Services		
	Sewage system	Waste collection	Drinking water
Costa	36.1%	62.7%	85.2%
Sierra	61.9%	64.2%	80.2%

Table 4 evidences that there is a lack of around 15-20% of drinking water in Costa and Sierra regions of Ecuador, and this percentage can increase to 30% in rural areas according to Ramírez et al., 2019, which implies that many Ecuadorians are consuming polluted water that increase the risk of contracting infectious diseases due to the toxicity of pollutants present in water (*e.g.* heavy metals). In addition, the deficiencies of sewage system and waste collection create sanitary consequences and generate a worse scenario to deal with water pollution. In fact, literature has placed Ecuador as the most harmed country in Latin America due to the contamination of aquatic environment (Harari & Harari, 2006). Therefore, in order to improve these aspects, several remediation programs have been implemented in the country, like “Programa Agua Segura y Saneamiento Para Todos”. This is a national program funded by Ministerio de Economía y Finanzas (MEF) and Banco de Desarrollo del Ecuador (BDE) aiming at improving the quality, coverage and continuity of drinking water services and sanitation through the funding of projects that guarantee human rights to water and sanitation (BDE, 2017).

Even though many programs for controlling the water pollution are being carried out in Ecuador, the existence of contaminated aquatic environments due to heavy metal and other contaminants still poses serious concern. Therefore, there is a necessity of developing greener and sustainable solutions for the effective treatment of polluted water, considering the biodiversity of Ecuador.

### 3. Hypothesis, General and Specific Objectives

#### 3.1. Hypothesis

Untreated cellulose extracted from Ecuadorian natural sources can be a solution to reduce the concentration levels of heavy metals present in polluted water. These natural cellulose particles exhibit suitable physicochemical properties for capturing copper (II) ions.

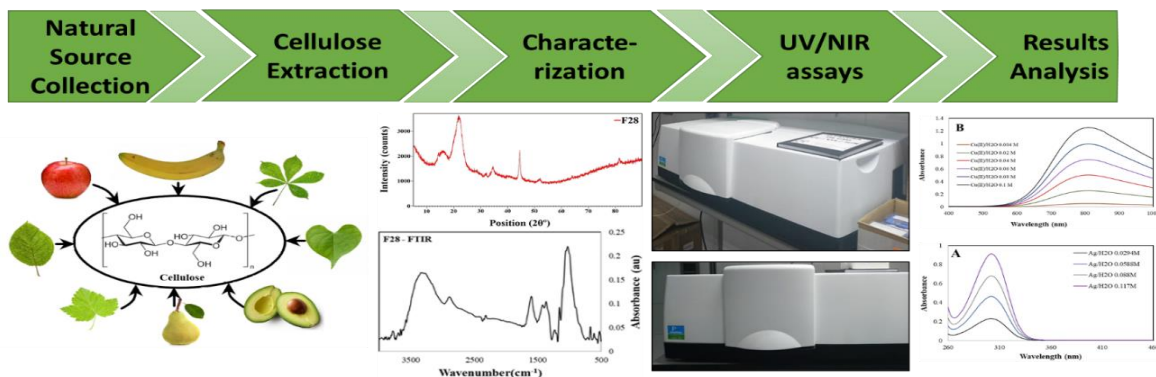
#### 3.2. General Objective

To extract from different Ecuadorian natural sources cellulose particles capable of capturing heavy metal ions, through standard extraction protocols, followed by characterization and tests to monitor their physicochemical properties and evaluate their efficiency.

#### 3.3. Specific Objectives (Scheme 1)

- I. Test adsorption capacities of commercially available cellulose (*i.e.* cellulose microcrystals, CMC) as a control.
- II. Extract cellulose particles (*i.e.* F20, F25, F28 and T1) from Ecuadorian native plants and fruits by following standard protocol of chemical extraction of cellulose in order to remove lignin and hemicellulose residual molecules.
- III. Perform the physicochemical characterization of natural cellulose particles by using FTIR, XRD, SEM and BET techniques.
- IV. Perform the UV-Vis-NIR tests of Cu (II) and Ag (I) solutions non-treated and cellulose-treated to obtain important data about the adsorption capacity of samples.

#### Scheme 1. Flow-chart of the objectives of this research



## **4. Methodology**

### **4.1. Materials**

The cellulose samples F20, F25, F28 and T1 extracted from different Ecuadorian natural sources were obtained in the cities Ibarra and Urcuquí, Ecuador. The raw material of F20, F25 and F28 cellulose samples were obtained at Mercado Amazonas on Avenue Alfredo Perez Guerrero, Ibarra, in the section of vegetable and fruits. The raw material T1 was purchased at Mercado Urcuquí located on Antonio Ante Street, Urcuquí, in the fruit section. For cellulose extraction and heavy metal solutions (treated and non-treated), many laboratory equipment and materials are utilized including analytical balance, sonicator, vortex, centrifuge, and sterile assay tubes.

### **4.2. Cellulose samples preparation**

Cellulose extraction was carried out following established protocols of chemical extraction followed by acid/base treatment, bleaching, and multiple washings with water to remove residual chemicals. The same process was used for each sample to prevent any effect of the protocol on the cellulose property. Control sample of cellulose microcrystals (CMC) was supplied by Sigma-Aldrich. (detailed protocol is restricted in this thesis).

### **4.3. Cellulose samples characterization**

Purified cellulose samples were characterized by using several techniques such as Fourier-Transform Infrared Spectroscopy (FTIR), X-Ray Diffraction (XRD), and Scanning Electron Microscopy (SEM).

Fourier Transform Infrared Spectroscopy (FTIR) is a characterization technique commonly used in material and biomedical analyses to obtain an infrared spectrum of absorption, emission, photoconductivity of liquid, solid samples or gases (Dwivedi et al., 2017). Principle of working of FTIR involves the emission of a bright ray from an incandescent source of light within the infrared wavelength range (Alawam, 2014). FTIR data were recorded using Spectrum Spotlight 200 FTIR instrument (Perkin Elmer, USA). First a spectrum of the gold-plated sample holder was acquired as background, and then the spectra of the samples were collected. The wavenumber range for the analysis was between 4000 to 600  $\text{cm}^{-1}$  with a total number of scans of 36 and at a 4- $\text{cm}^{-1}$  resolution.

X-ray diffraction (XRD) is a powerful characterization technique of qualitative analysis of crystalline solids that exhibit long range order. It is based on the use of radiation produced by X-rays on a crystalline solid sample to observe the crystal lattice and determine the structure of the atoms and molecules. Thereby, XRD allows to distinguish the structural arrangement; even having the same elementary profile is possible to detect slight differences between different samples (Day, 2016). In this research, XRD patterns were gathered on an EMPYREAN diffractometer (PANalytical, NL) in a Bragg-Brentano configuration at 40kV and 45A and monochromatic X-rays of Cu K- $\alpha$  wavelength ( $\lambda = 1.541 \text{ \AA}$ ) using a Ni filter. The crystallinity index (CrI) was determined for each cellulose sample following the method described by Segal *et al.* using the equation (1):

$$\text{Equation (1): } CrI(\%) = \frac{I_{002} - I_{am}}{I_{002}} \times 100\%$$

Where  $I_{002}$  is the counter reading at peak intensity at a  $2\theta$  angle close to  $22^\circ$  representing crystalline material,  $I_{am}$  is the counter reading at peak intensity at a  $2\theta$  angle close to  $18^\circ$  and stands for the amorphous material (Costa et al., 2015; Roncero Vivero, 2000).

Finally, Scanning Electron Microscopy (SEM) is considered as one of the most versatile tools to study and analyse the microstructure morphology and chemical composition (Zhou, Apkarian, & Wang, 2006). SEM was used in this investigation in order to image the surface structure and morphology of cellulose samples, for the posterior analysis of physico-chemical properties related to the reduction of heavy metal concentrations in prepared solutions. SEM observations of the different cellulose samples were examined by using a MIRA 3 (TESCAN, CZ) Field Emission Gun Scanning Electron Microscope (FEG-SEM). Pore size distributions were determined using Density Functional Theory (DFT) and the calculated specific surface areas were deduced from the Brunauer–Emmett–Teller (BET) equation.



#### 4.4. Aqueous solutions of heavy metals

Heavy metals tested in this research include copper (II) and silver (I), and were obtained from sources such as copper sulphate pentahydrate from Sigma-Aldrich and silver nitrate purchased from Novaquem and Representaciones Venegas, respectively. Heavy metal precursors were diluted in water and many different concentrations were prepared for each heavy metal source (Table 5). Equipment such as analytical balance and vortex were used for the preparation.

**Table 5. Concentrations of heavy metal solutions**

[Cu(II)/H <sub>2</sub> O] (M)	[Ag(I)/H <sub>2</sub> O] (M)
0.004	0.029
0.02	0.058
0.04	0.088
0.06	0.117
0.08	
0.1	

Heavy metal concentrations lower than the concentrations listed in Table 5 are difficult to measure using UV-Vis-NIR equipment, and greyer  values of concentrations were prepared and measured to have more data to obtain the calibration curve.

#### 4.5. Cellulose-treated solutions

Purified cellulose samples after characterization and commercially available cellulose (i.e. CMC) were used to prepare cellulose-treated solutions, which contain a certain amount of cellulose sample in the different heavy metal solutions previously prepared. 1 and 10 mg of CMC, F20 and F28 were tested on each 10 mL heavy metal solution in triplicate. Moreover, 1 mg of F25 and 10 mg of T1 were taken and placed in the different 10 mL heavy metal solutions in triplicate. Permanence time of cellulose in solution was not evaluated in this research.

#### 4.6. UV-Vis-NIR assays

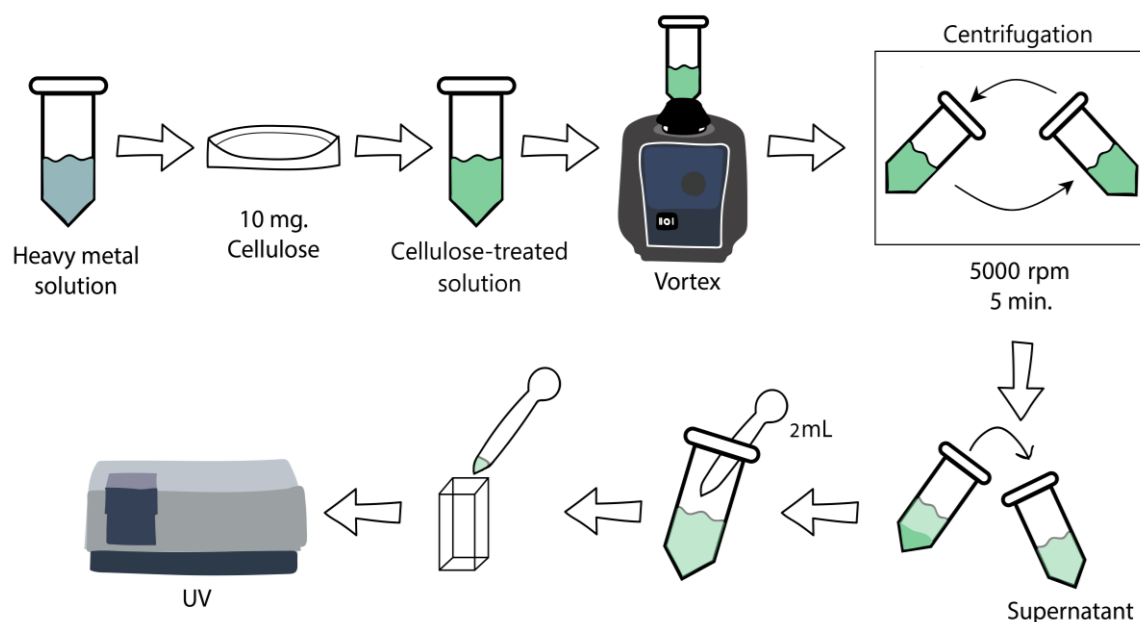
Ultraviolet-Visible-Near Infrared (UV-Vis-NIR) spectroscopy is a widely used tool for qualitative and quantitative characterization and analysis of materials and solutions. UV-Vis-NIR is sensitive for aqueous solutions due to transparency of water in the spectral region between 200 and 800 nm. In the UV range, absorption coefficients can be considerably high, therefore sensitivity is outstanding (Dai et al., 2016). In this research, different wavelength ranges were used depending on the heavy metal source to be measured. Heavy metal solutions were directly measured in a LAMBDA 1050 UV-Vis-NIR spectrophotometer (Perkin Elmer, USA). In contrast, cellulose-treated solutions needed to be vortexed, centrifuged and, to avoid possible interference of any residual cellulose particles, supernatant was placed in other assay tube (Scheme 2). Then, 2 mL of the liquid supernatant was placed in a quartz cuvette and measured in the UV-Vis-NIR equipment at maximum wavelength. Pellets of samples were stored for future research and analysis.

Reduction percentages of copper in cellulose-copper suspensions were readily calculated by using the Lambert-Beer Law illustrated in equation (2) and the maximum absorbance of characteristic absorption peaks of heavy metals.

$$\text{Equation (2): } A = \varepsilon \cdot l \cdot C$$

In equation (2),  $A$  stands for the absorbance value,  $\varepsilon$  is a constant value that represents the molar absorptivity,  $l$  is the length of cuvette the light is passing through, and  $C$  is the concentration of the solution associated with the absorbance measured. According to equation (2), absorbance is directly proportional to the concentration, which means that any decrease in absorbance will result from a reduction in the concentration (Swinehart, 1962).

## Scheme 2. Flow-chart of the UV-Vis-NIR procedure for cellulose-treated suspensions



### 4.7. Statistical analysis

The research project results are statistically analysed by using an ANOVA model of two factors considering two types of effects: first and second order, by using the equation (3):

$$\text{Equation (3): } y = \mu + a + b + (a * b)$$

In equation 3,  $\mu$  stands for mean,  $a$  is the effect of the cellulose sample (different precursors: CMC, F20, F25, F28 and T1),  $b$  is the effect of the amount of cellulose used (1 and 10 mg/mL) and  $a * b$  is the interaction between both factors and its effect on the adsorption capacities of cellulose. The second ( $a$ ) and third ( $b$ ) terms in equation 3 are first order effects, whereas the last term ( $a * b$ ) is second order effect. Since three different concentrations of copper (II) were tested (0.004 M, 0.02 M and 0.04 M), one ANOVA assay was performed separately for each set of results. ANOVA model is applied to know whether there is a significant difference between the means of the adsorption capacities parameter of isolates compared with control sample (CMC). In addition, Honest Significant Difference (HSD) Tukey test was conducted for each first order factors. This test allows to have a thorough analysis of the influence of those

parameters on the adsorption capacities of cellulose samples. For the statistical analysis (ANOVA and HSD Tukey), a significance level of  $p > 0.05$  was considered. R-studio software was used for ANOVA and HSD Tukey tests (agricolae package), and regression analysis of calibration curves for heavy metal solutions was carried out using Microsoft Excel.

## 5. Results

### 5.1. Characterization of commercially available cellulose (i.e. Cellulose Micro-Crystals (CMC)) as a control

The Fourier Transform-Infrared (FTIR) spectrum of commercial CMC sample, illustrated in Figure 1, indicates characteristic peaks for cellulose including C-C, C-OH, C-H ring and side group vibration bands which clearly arise at  $\sim 1000 \text{ cm}^{-1}$ , and also C-O-C glycosidic ether band notably appear at  $\sim 1105 \text{ cm}^{-1}$ . Additionally, important peaks are evident at  $\sim 1300 \text{ cm}^{-1}$ ,  $\sim 1600 \text{ cm}^{-1}$ ,  $\sim 2900 \text{ cm}^{-1}$ , and  $\sim 3300 \text{ cm}^{-1}$  which correspond to  $\text{CH}_2$  rocking vibrations at C6 band, OH bending of adsorbed water,  $\text{sp}^3$  C-H stretching and OH stretching frequencies, respectively (Auta et al., 2017).

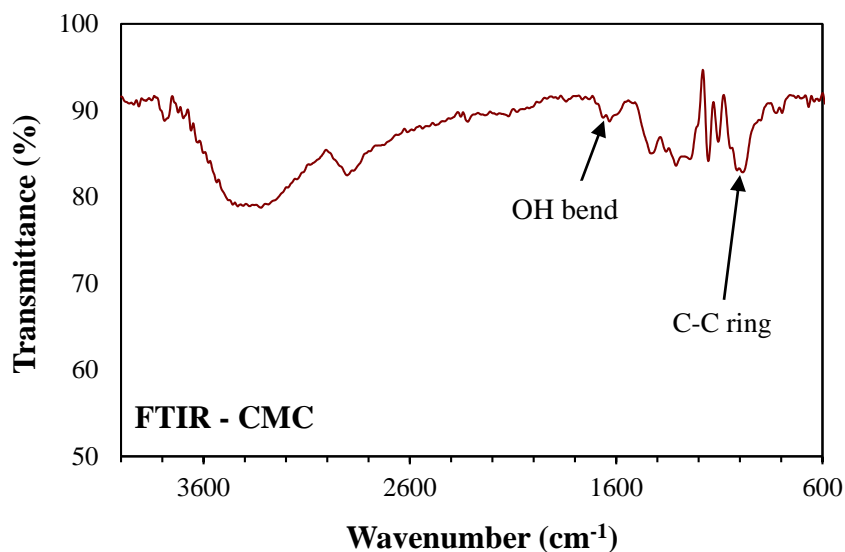


**Figure 1.** FTIR spectrum of the control sample: Cellulose microcrystals

Generally, cellulose composition includes crystalline and amorphous phases. The XRD pattern of the control sample CMC and the peaks intensity (Figure 2) exhibits a well-

defined main peak around  $2\theta = 22^\circ$ . Using equation (1), a crystallinity index of 78.1% is deduced.

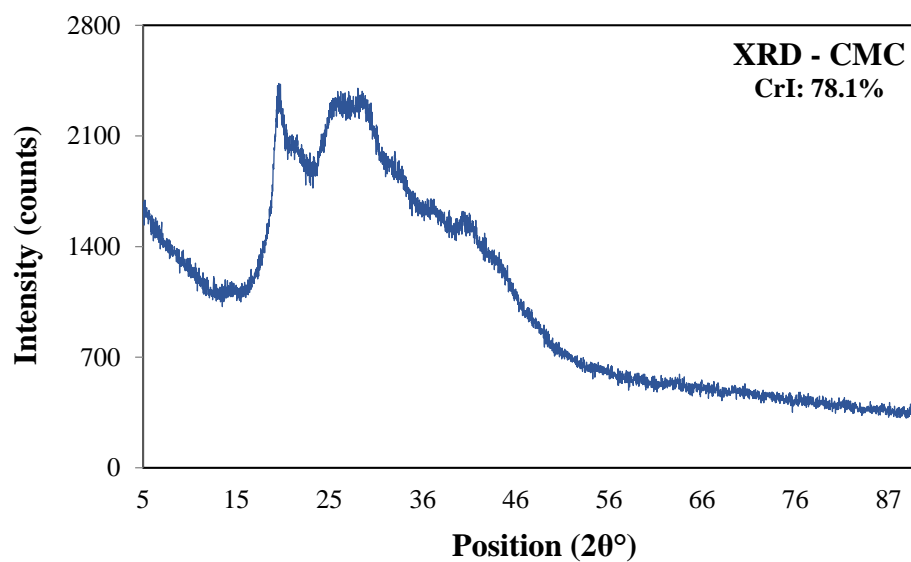


**Figure 2.** XRD pattern of the control sample: Cellulose microcrystals

SEM observations of commercially available cellulose (CMC), displayed in Figure 3, showed that surface structure of CMC presents roughness similar to a tree bark formation and its morphology is slightly tubular.

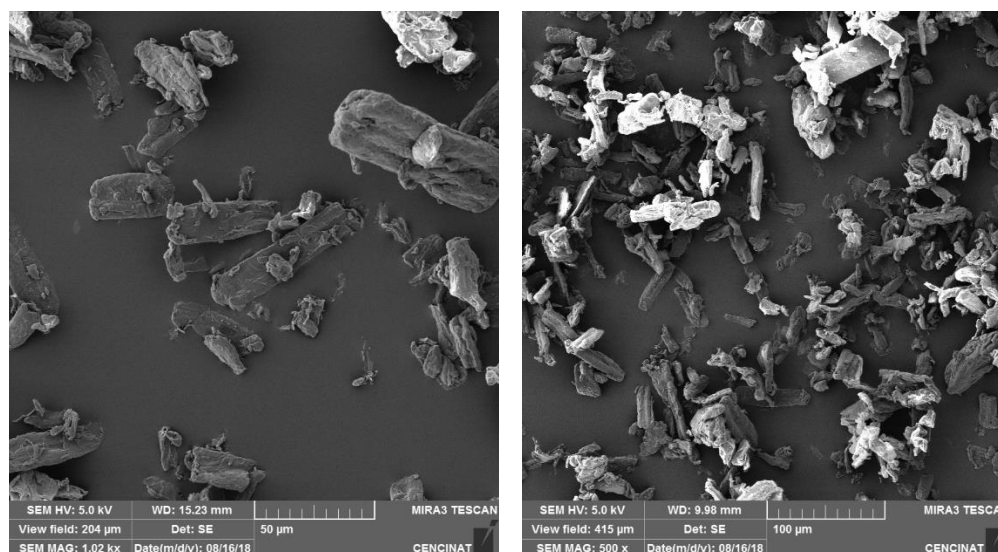


**Figure 3.** SEM micrographs of the control sample: Cellulose microcrystals

## 5.2. Characterization of cellulose samples extracted from natural sources

It is important to remark that natural cellulose particles were extracted from different biodiverse sources using the same extraction process to prevent any possible effects of the extraction on their physicochemical properties. Cellulose exhibited various physicochemical properties, as shown in Figure 4. FTIR spectra were useful to identify cellulose content and residual molecules of cellular wall components, such as hemicellulose or lignin.

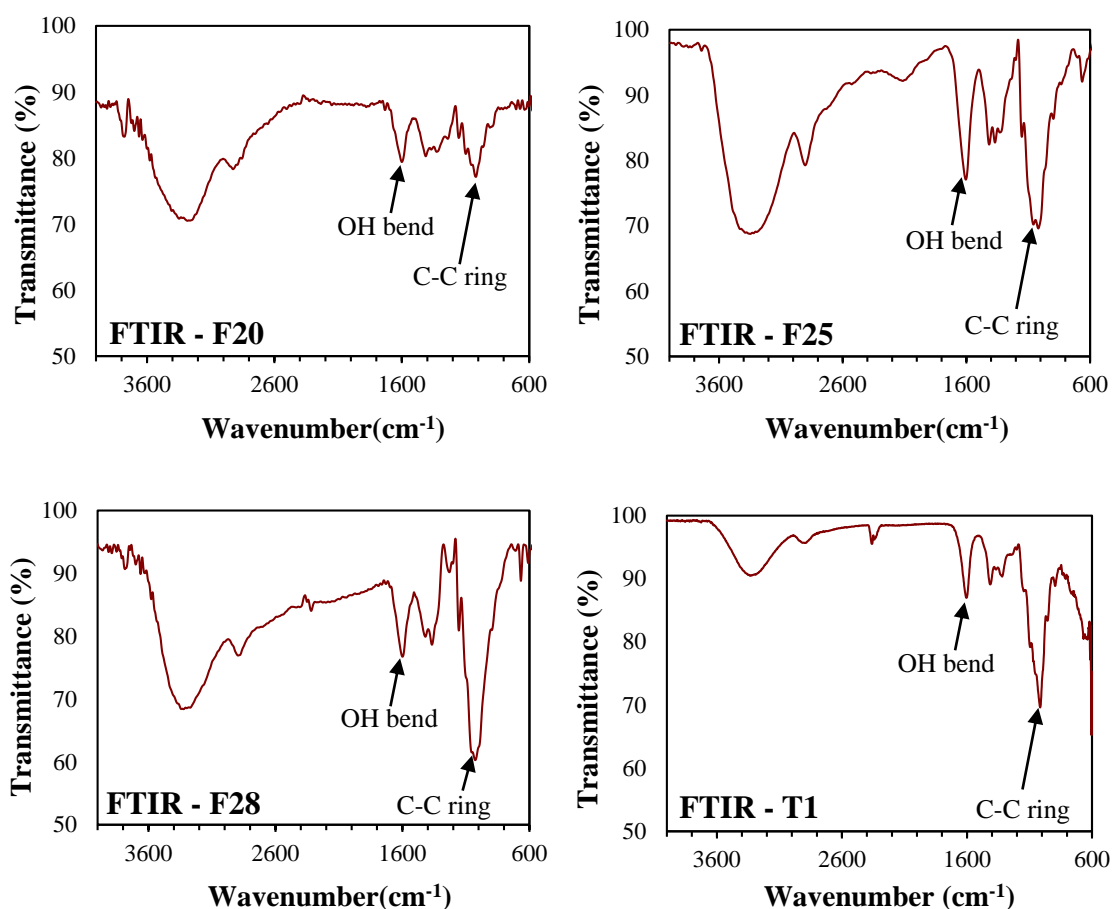


**Figure 4.** FTIR spectra of F20, F25, F28 and T1 cellulose samples

X-ray diffraction (XRD) tests on the four cellulose samples depicted distinct graphs and different degrees of crystallinity (Figure 5). The major peaks around  $2\theta = 20 - 25^\circ$  are attributed to cellulose crystalline structure, while the peaks around  $2\theta = 15 - 18^\circ$ , represents the samples amorphous region (Segal, Creely, Martin, & Conrad, 1959).

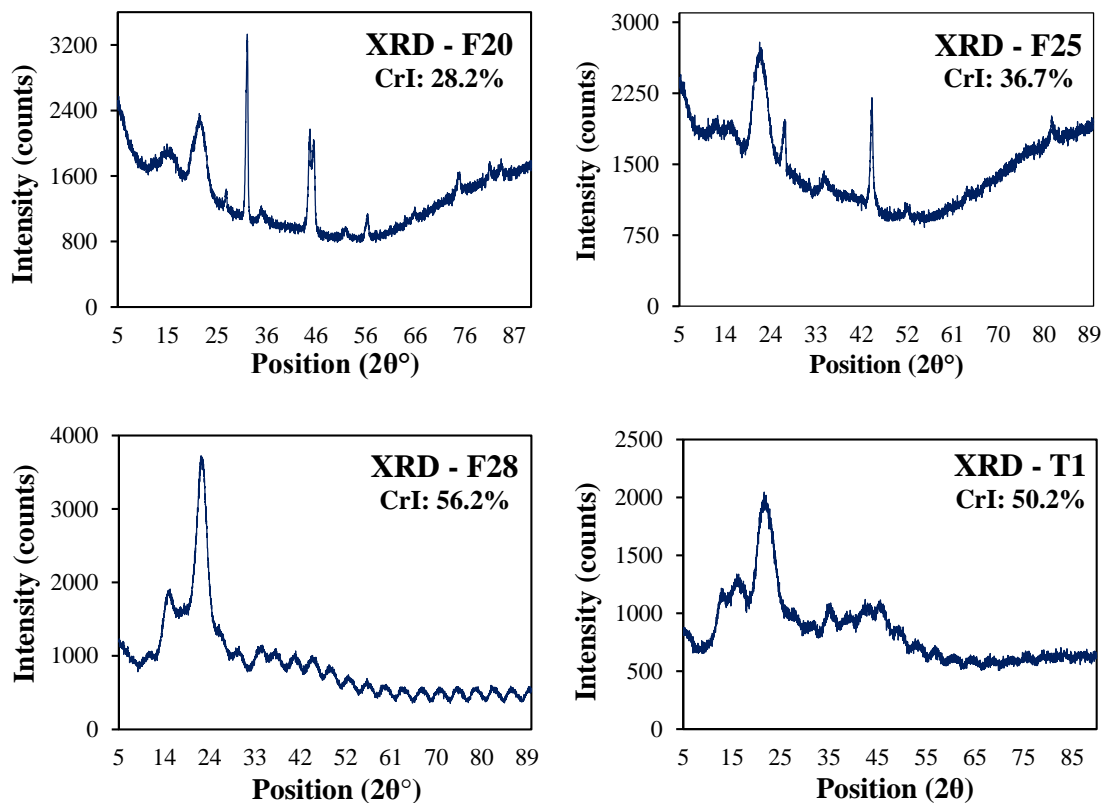


**Figure 5.** XRD patterns of F20, F25, F28 and T1 cellulose samples

Scanning Electron Microscopy (SEM) pictures of the new isolates, illustrated in Figures 6-9, reveal that each cellulose sample presents a unique morphology, porosity, and size despite that the same extraction process was used for all samples. As displayed in Fig 6 and 8, the external structure of F20 and F28 fibers are porous with an irregular surface presenting roughness. Figures 7 and 9 show that F25 and T1 samples present a more compact surface and similar degree of porosity compared with F20 and F28 samples.

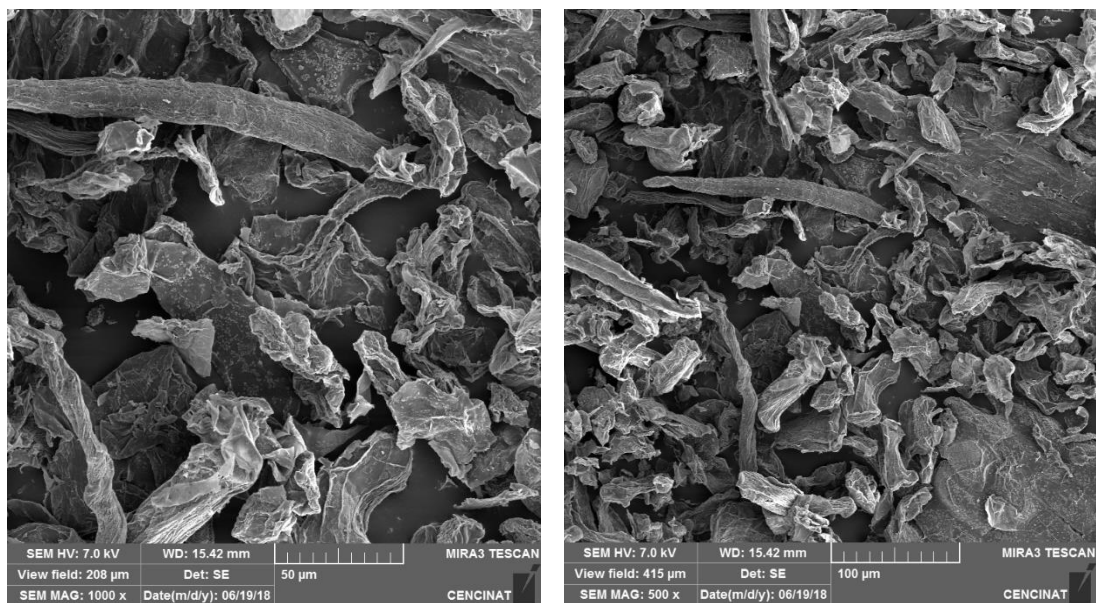


**Figure 6.** SEM micrographs of F20 cellulose Sample

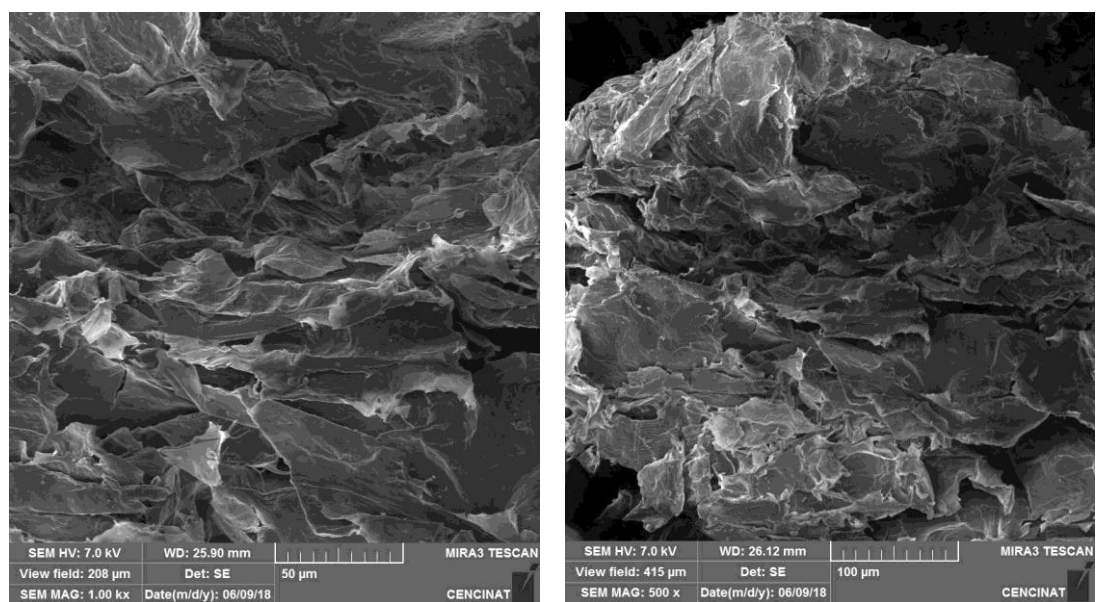


**Figure 7.** SEM micrographs of F25 cellulose sample



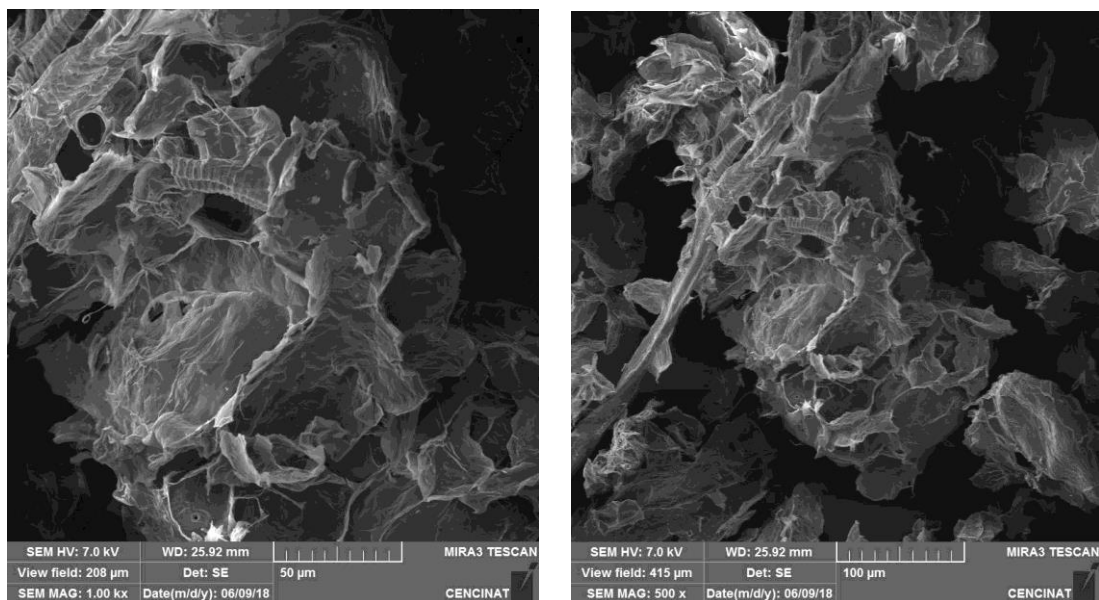


**Figure 8.** SEM micrographs of F28 cellulose sample

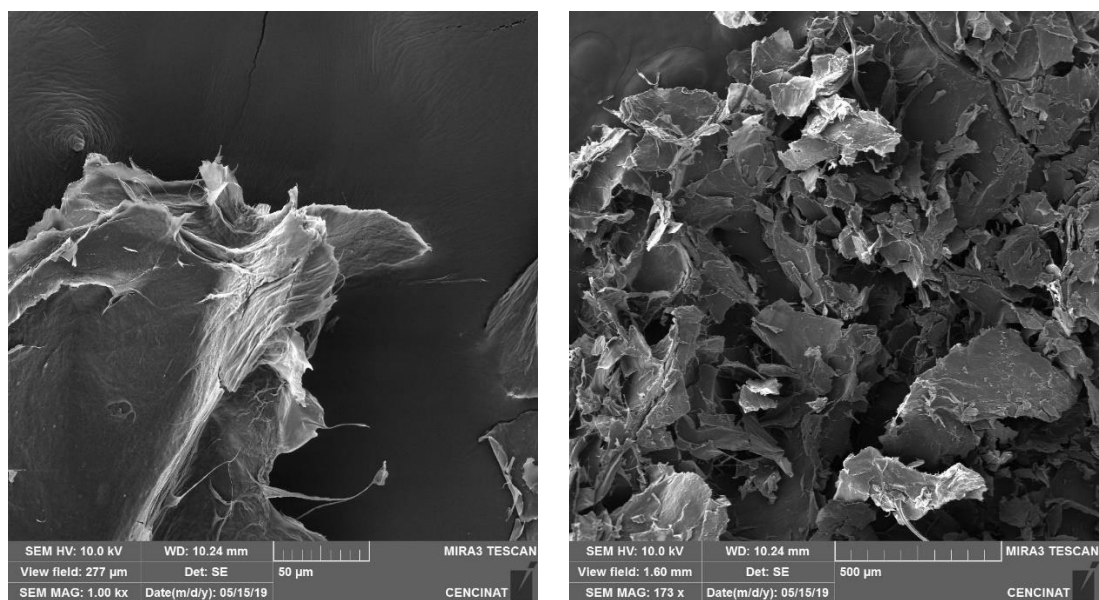


**Figure 9.** SEM micrographs of T1 cellulose sample

### 5.3. UV-Vis-NIR assays on standard heavy metal solutions.

Maximum values of absorbance for each peak depicted on UV-Vis-NIR absorption spectra served as a reference for the posterior measurements of cellulose-treated heavy metal solutions. For the evaluation of adsorption capacities of cellulose samples, the three solutions with the lowest concentration were tested, therefore the characteristic peaks of

copper solutions presented in Figure 10 correspond to 0.004 M, 0.02 M and 0.04 M solutions.

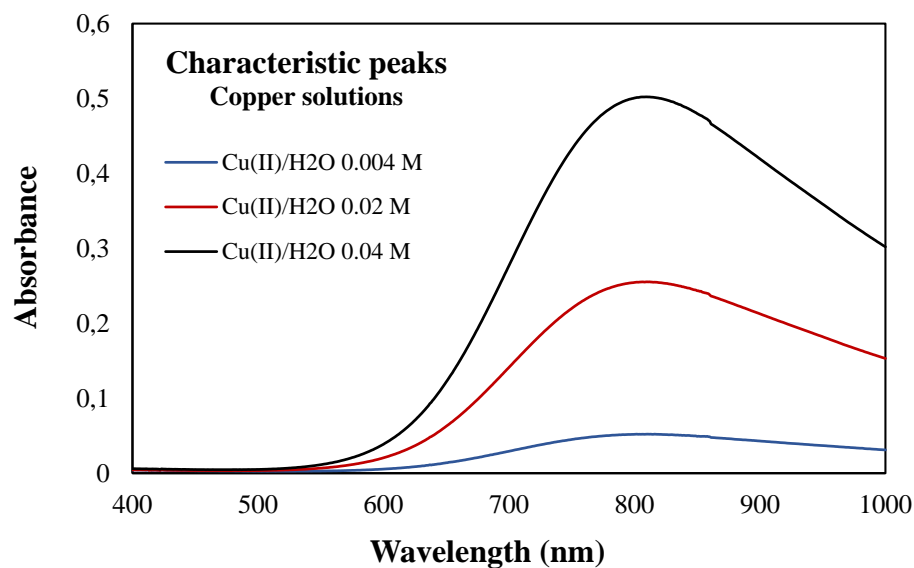


**Figure 10.** Absorption spectra of copper aqueous solutions

As mentioned in methodology, 4.4 section, extra solutions of heavy metals were prepared in order to have more data to obtain the calibration curve. Calibration curve of copper standard solutions obtained from UV-Vis-NIR measurements was set at maximum wavelength, which is 813 nm, as shown in Figure 11.

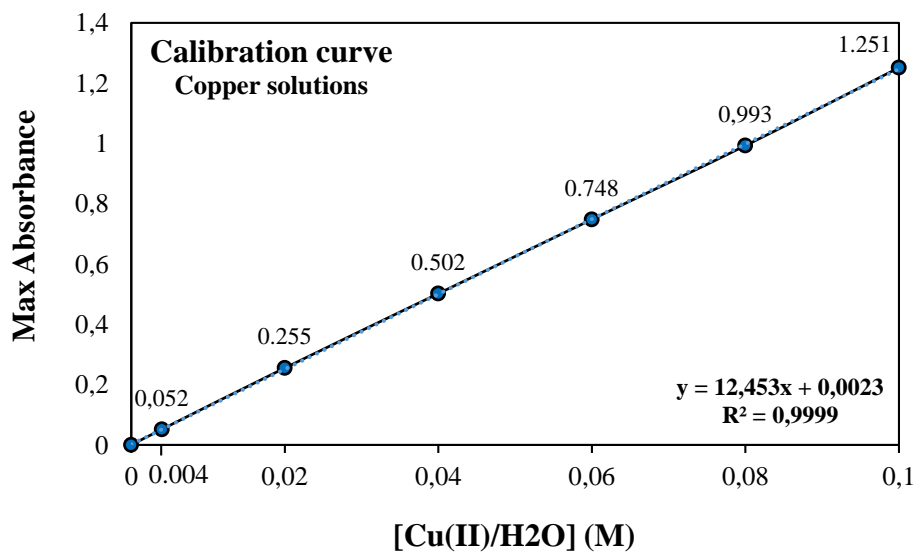


**Figure 11.** Calibration curve of copper standard solutions (max wavelength: 813 nm)

In the case of silver solutions, the characteristic peaks evaluated correspond to silver standard solutions with the lowest concentration, which are 0.029 M, 0.059 M and 0.088 M solutions. UV-Vis-NIR absorption spectra of those solutions is presented in Figure 12.

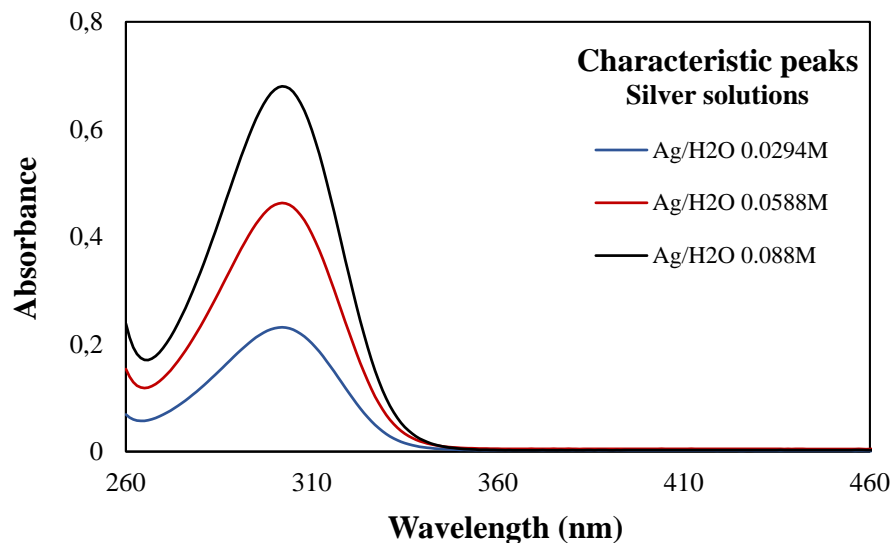


**Figure 12.** Absorption spectra of silver aqueous solutions

For the obtainment of the calibration curve of silver standard solutions, one more solution was prepared with a concentration of 0.117 M. Calibration curve of those solutions was set at the maximum wavelength, which is 302 nm, as shown in Figure 13.

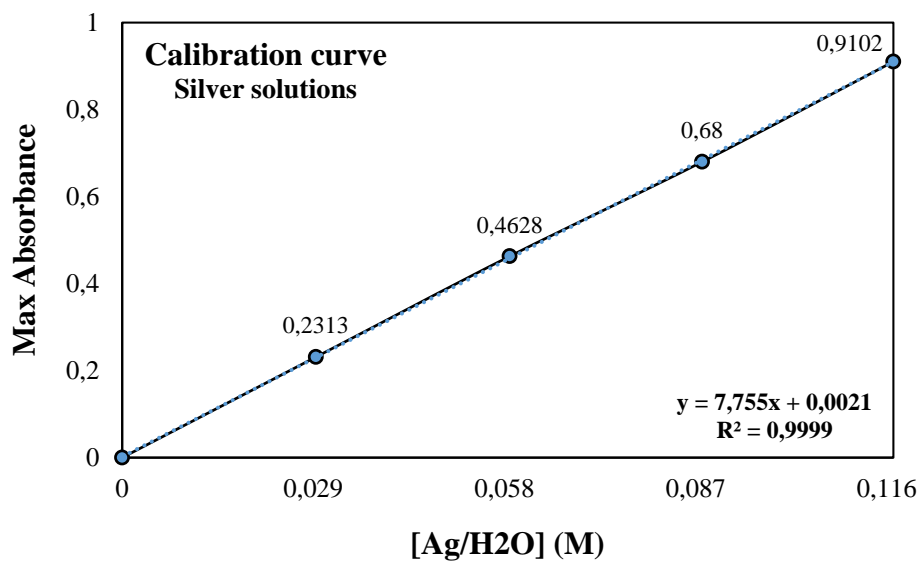


**Figure 13.** Calibration curve of silver standard solutions (max wavelength: 302 nm)

#### 5.4. Percentages of removal of copper in cellulose-copper adsorption assays

Copper remaining in CMC-copper suspensions is presented as only one bar which involves every single copper concentration in contact with 1 and 10 mg/mL of CMC, respectively. Each of these analyses were carried out in triplicate, as shown in Annex A. Most of the values of absorbance of CMC-copper suspensions are above the values of the detection limits and lower values presented a slight difference, therefore they were negligible. There was no standard deviation for CMC, since it depicted no adsorption capacities in all tests (100% copper remaining in each measurement).

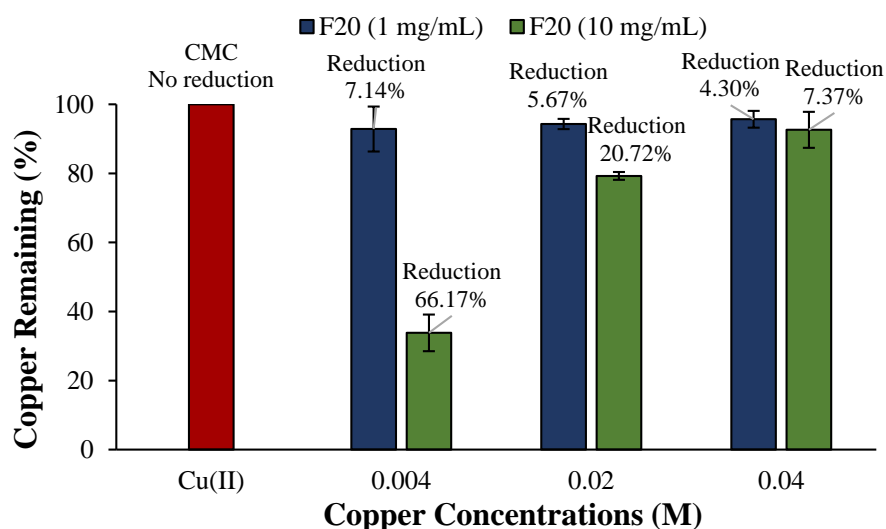


**Figure 14.** Percentages of removal of copper in F20-copper suspensions

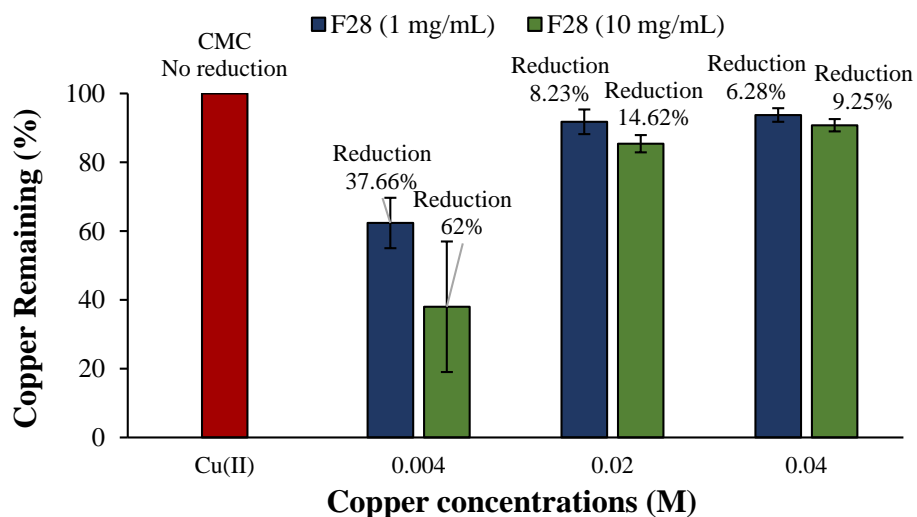


**Figure 15.** Percentages of removal of copper in F28-copper suspensions

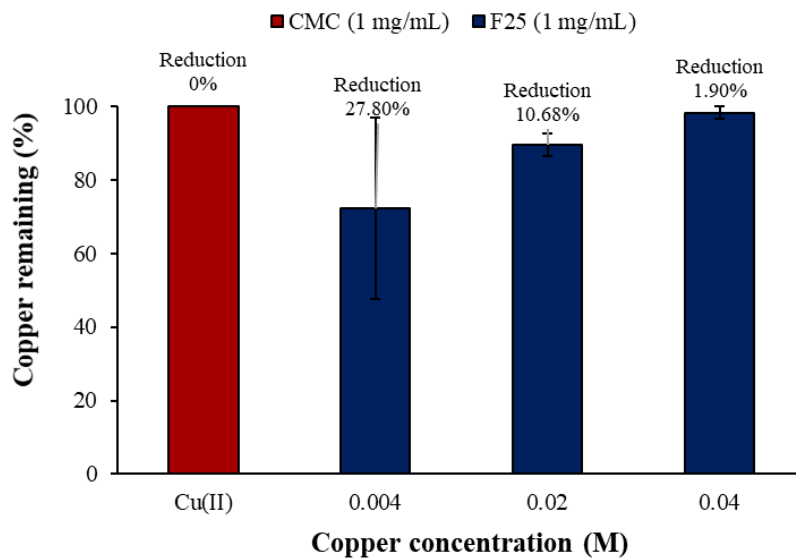


**Figure 16.** Percentages of removal of copper in F25-copper suspensions

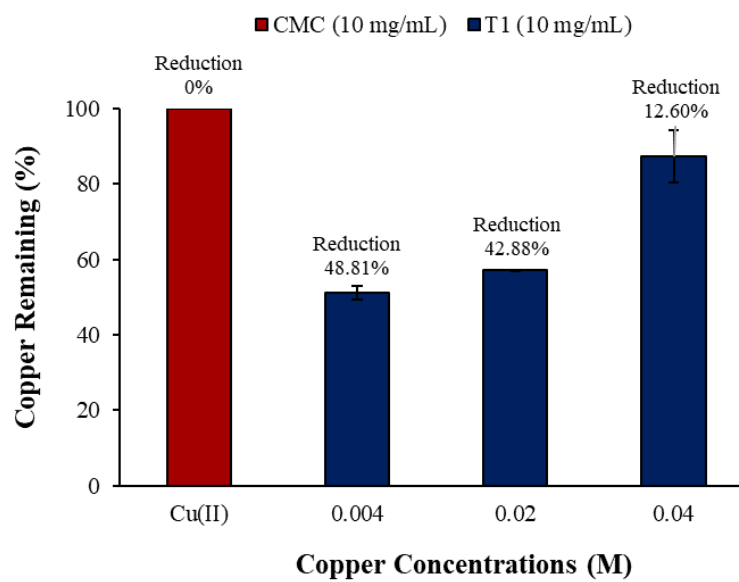


**Figure 17.** Percentages of removal of copper in T1-copper suspensions

### 5.5. Statistical analysis

Results of ANOVA by using the equation (3) allow to compare the mean different adsorption capacities of cellulose particles, in order to establish whether a difference exist or not. Considering the probability shown in Table 6, at least one of the treatments (cellulose samples) differs from the controls. Furthermore, the Table 6 indicates that the same behavior is depicted regarding the amount of cellulose.

**Table 6. ANOVA of the absolute concentration values of copper-cellulose suspensions (0.004 M)**

ANOVA of absolute concentration values of 0.004 M cellulose-copper mixtures						
	Df	Sum Sq	Mean Sq	F value	Pr(>F)	
Treatment	4	1.57E-05	3.93E-06	16.54	1.54E-05	***
Amount	1	4.76E-06	4.76E-06	20.01	0.000384	***
Treatment:Amount	2	4.76E-06	2.38E-06	10	0.001522	**
Residuals	16	3.80E-06	2.38E-07			

Signif. codes: 0 '\*\*\*' 0.001 '\*\*' 0.01 '\*' 0.05 '.' 0.1 ' ' 1

The validation graphs obtained from ANOVA model of values of absolute concentration (Annex A) of cellulose-copper suspensions with an initial concentration of 0.004 M are displayed in Figure 18. The first validation graph permits to have a better idea of the normality of the residuals. Furthermore, the normality graph depicted shows that the majority values lies over the theoretical behavior line. Figure 18 C displays a linear correlation between measured and predicted values.

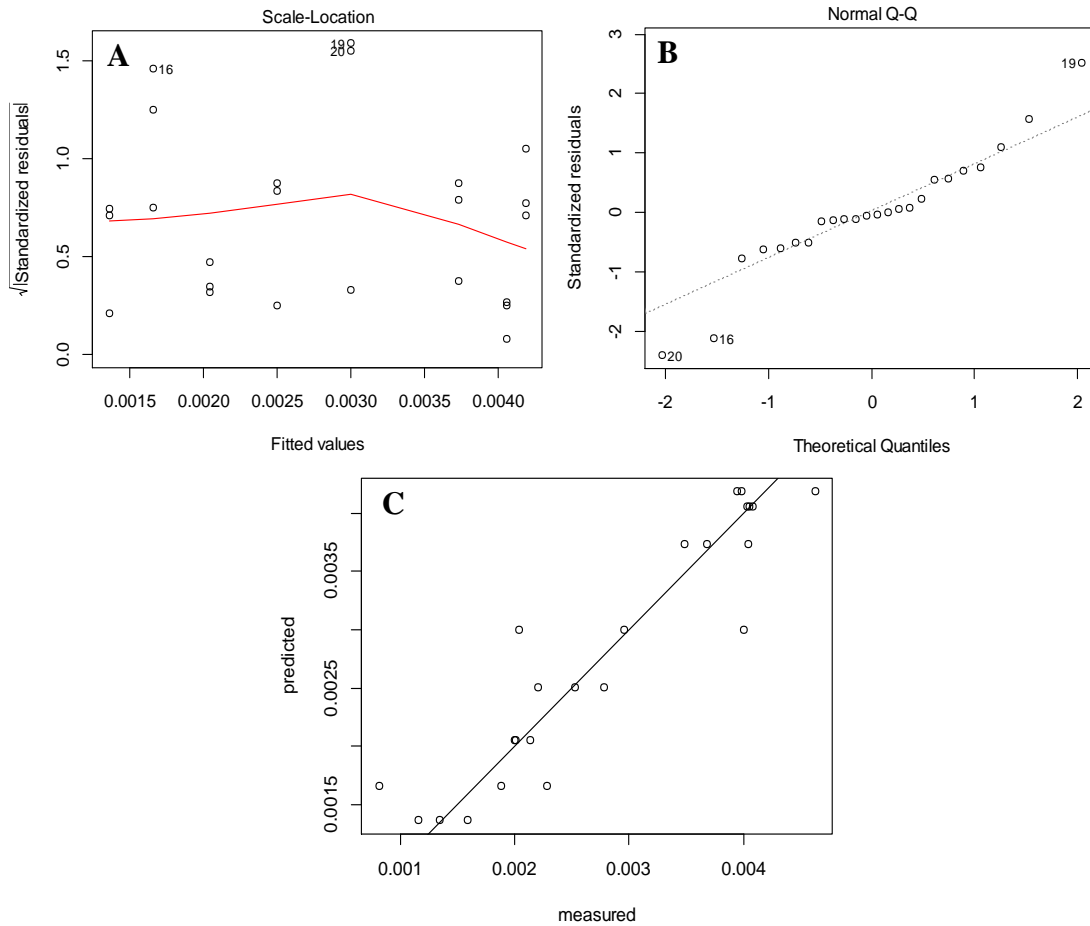


**Figure 18.** Validation graphs of (A) square root of the standardized residuals and the fitted values, (B) the standardized residuals and the theoretical quantiles, and (C) measured vs predicted values of ANOVA of cellulose-copper suspensions (0.004 M).

The adsorption capacities vary according to the cellulose sample used and the supplied amount of cellulose on cellulose-copper suspensions. In fact, HSD Tukey tests present statistic information about the influence of those parameters on the values of absolute concentration (Annex B) in cellulose-copper suspensions with an initial concentration of 0.004 M, as noticed in Figure 19.

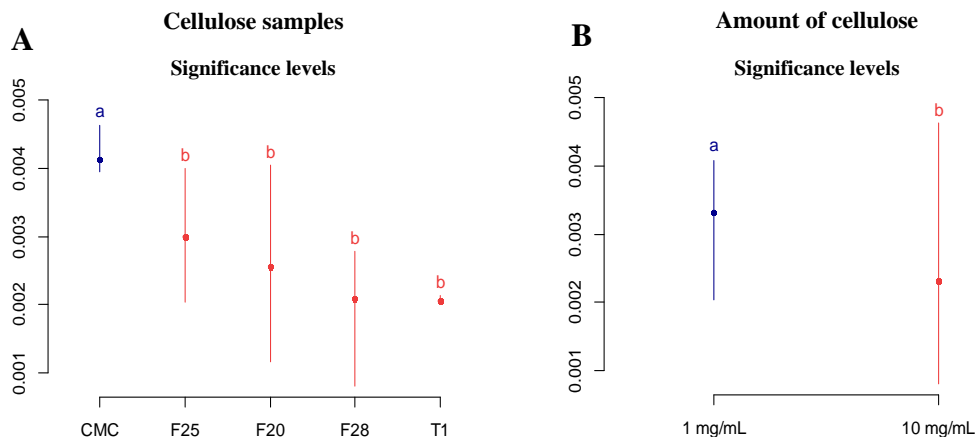


**Figure 19.** Significance differences among the means of first order effects. (A) Cellulose samples, and (B) amount of cellulose used in cellulose-copper suspensions (0.004 M).

Similarly, ANOVA on cellulose-copper suspensions with an initial concentration of 0.02 M was conducted. Data obtained from ANOVA model is illustrated in Table 7. Significance codes in Table 7 prove that the interaction of treatment (cellulose samples) and amount of cellulose, as well as the first order effects have a significant difference on the mean adsorption capacities of cellulose particles.

**Table 7. ANOVA of the absolute concentration values of copper-cellulose suspensions (0.02 M)**

ANOVA of absolute concentration values of 0.02 M cellulose-copper mixtures						
	Df	Sum Sq	Mean Sq	F value	Pr(>F)	
Treatment	4	1.50E-04	3.75E-05	233.58	5.72E-14	***
Amount	1	9.37E-06	9.37E-06	58.42	9.97E-07	***
Treatment:Amount	2	6.71E-06	3.35E-06	20.92	1.60E-07	***
Residuals	16	2.57E-06	1.60E-07			

Signif. codes: 0 '\*\*\*' 0.001 '\*\*' 0.01 '\*' 0.05 '.' 0.1 ' ' 1

Figure 20 illustrates the validation graphs of square root of standardized residuals and fitted values, standardized residuals and theoretical quantiles, and the measured against



the predicted values of ANOVA model carried out on values of absolute concentration of cellulose-copper solutions (0.02 M).

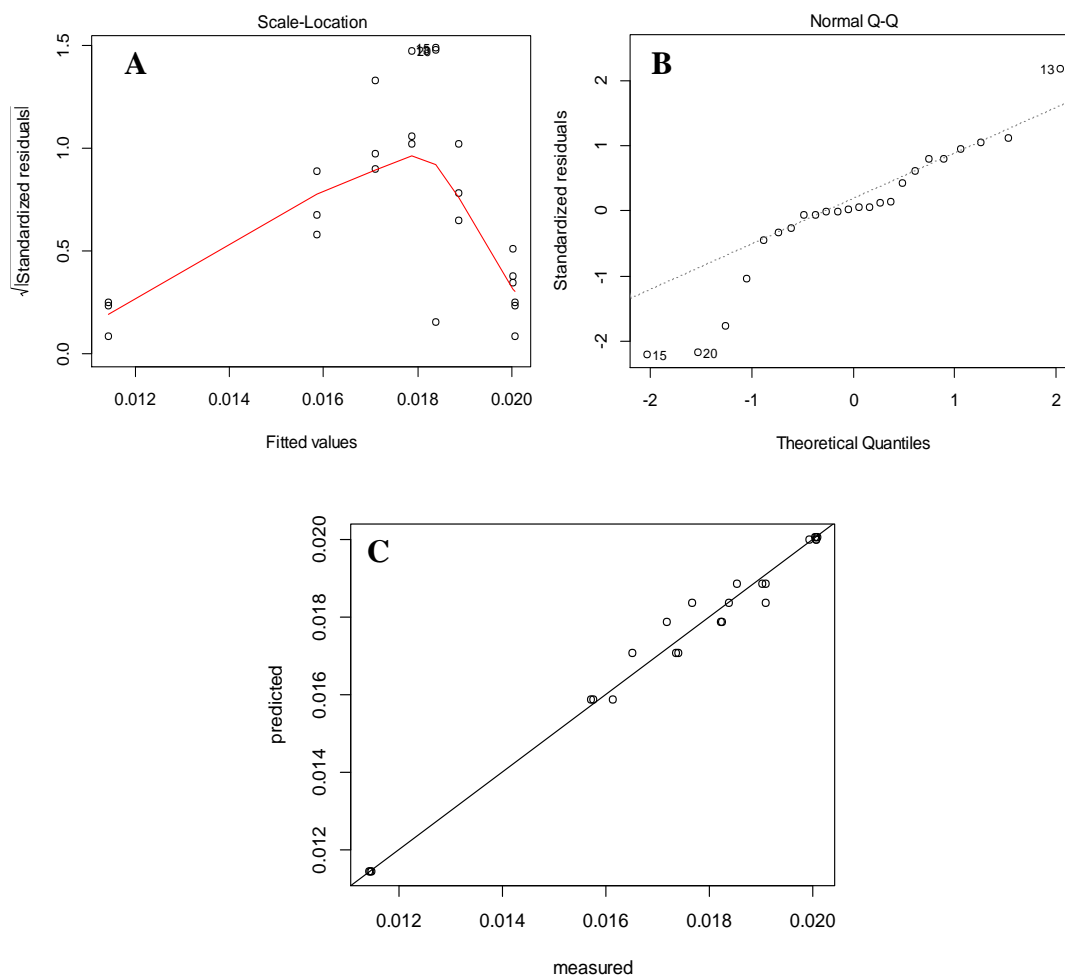


**Figure 20.** Validation graphs of (A) square root of the standardized residuals and the fitted values, (B) the standardized residuals and the theoretical quantiles, and (C) measured vs predicted values of ANOVA of cellulose-copper suspensions (0.02 M).

HSD Tukey tests present statistic information about the influence of first order effects on values of absolute concentration (Annex B) in cellulose-copper suspensions with an initial concentration of 0.02 M. As shown in Figure 21, there are significant differences between the cellulose samples used. T1 exhibits the highest significant difference compared with control (CMC) samples and the other cellulose samples. Additionally, the amount of cellulose used has a significant effect on the adsorption capacities of cellulose.

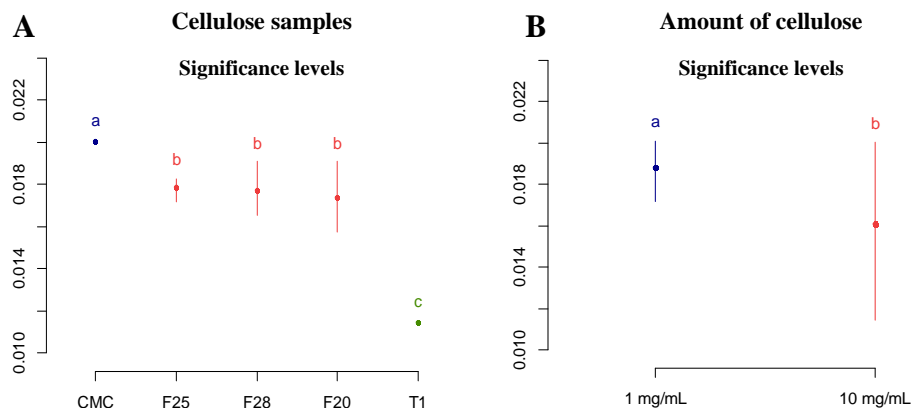


**Figure 21.** Significance differences among the means of first order effects. (A) Cellulose samples, and (B) amount of cellulose used in cellulose-copper suspensions (0.02 M).

Finally, ANOVA model applied in the set of values of absolute concentration of cellulose-copper suspensions with an initial concentration of 0.04 M reveals the information illustrated in Table 8, which indicates that only the type of cellulose influence on the adsorption capacities. In contrast, amount of cellulose and its interaction effect with treatment factor do not exhibit any type of influence on the adsorption properties of cellulose particles.

**Table 8.** ANOVA of the absolute concentration values of copper-cellulose suspensions (0.04 M)

ANOVA of absolute concentration values of 0.04 M cellulose-copper mixtures						
	Df	Sum Sq	Mean Sq	F value	Pr(>F)	
Treatment	4	6.45E-05	1.61E-05	8.731	6.16E-04	***
Amount	1	2.97E-06	2.97E-06	1.608	0.222879	
Treatment:Amount	2	1.31E-06	6.53E-07	0.354	0.707439	
Residuals	16	2.96E-05	1.85E-06			

Signif. codes: 0 '\*\*\*' 0.001 '\*\*' 0.01 '\*' 0.05 '.' 0.1 ' ' 1

The validation graphs obtained by plotting the ANOVA model used for cellulose-copper suspensions (0.04 M) are presented in Figure 22.

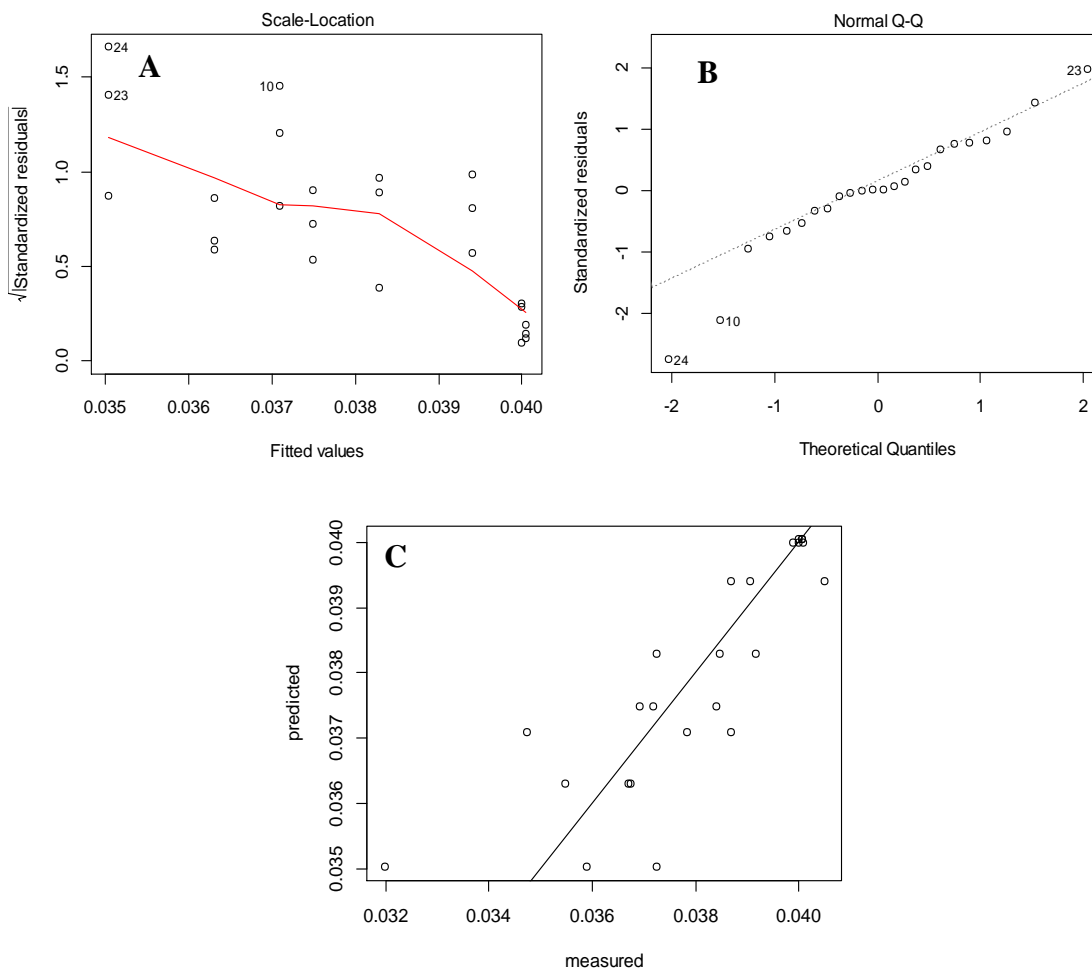


**Figure 22.** Validation graphs of (A) square root of the standardized residuals and the fitted values, (B) the standardized residuals and the theoretical quantiles, and (C) measured vs predicted values of ANOVA of cellulose-copper suspensions (0.04 M).

Further analyses of factors that affects the values of absolute concentration in cellulose-copper suspensions with an initial concentration of 0.04 M were carried out by using HSD Tukey test. As seen in Figure 23 A, T1 emerges as the cellulose sample with the highest significant difference compared with control (CMC) sample. On the other hand, Figure 23 B suggests that there is a significant difference when using a higher amount of cellulose.

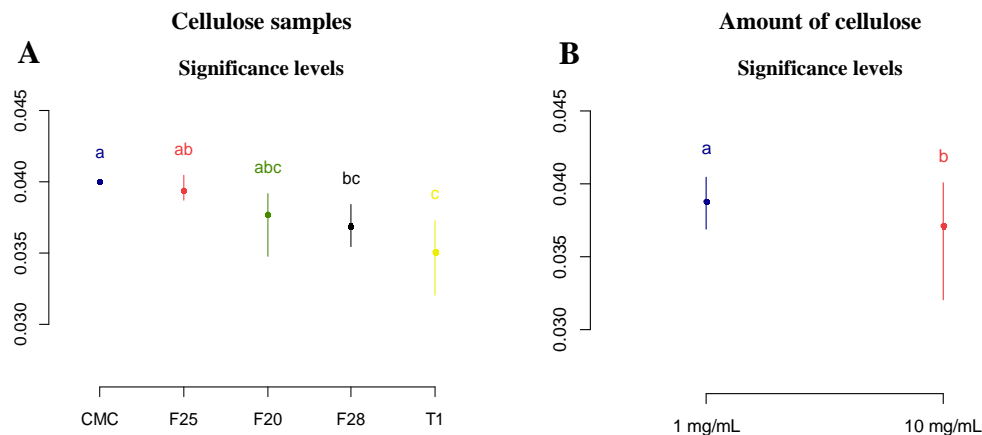


**Figure 23.** Significance difference among first order factors. **A)** Cellulose samples, and **B)** amount of cellulose used in cellulose-copper suspensions (0.04 M).

Statistical analysis of copper remaining percentages including means and standard deviations are presented in Tables 9 and 10 based on data collected from UV-Vis-NIR measurements for each cellulose-copper suspension.

**Table 9.** Statistical analysis (mean, standard deviation, coefficient of variation (CV) and statistical significance) of copper remaining percentages for the different cellulose-copper suspensions using 1 mg/mL of cellulose samples.

Cellulose samples (1mg/mL)		Copper remaining (%)		
		0.004 M	0.02 M	0.04 M
CMC	Mean	100	100	100
	Std. Deviation	0	0	0
F20	Mean	92.86	94.33	95.7
	Std. Deviation	6.51	1.48	2.43
	CV (%)	7.01	1.57	2.54
Sig. probability		0.137	0.003	0.038
CMC	Mean	100	100	100
	Std. Deviation	0	0	0
F25	Mean	72.2	89.32	98.1
	Std. Deviation	24.54	3.06	1.7
	CV (%)	33.99	3.43	1.73
Sig. probability		0.152	0.004	0.126
CMC	Mean	100	100	100
	Std. Deviation	0	0	0
F28	Mean	62.34	91.77	93.72
	Std. Deviation	7.33	3.58	1.99
	CV (%)	11.76	3.90	2.12
Sig. probability		0.001	0.017	0.005

**Table 10. Statistical analysis (mean, standard deviation, coefficient of variation (CV) and statistical significance) of copper remaining percentages for the different cellulose-copper suspensions using 10 mg/mL of cellulose samples.**

Cellulose samples (10mg/mL)		Copper remaining (%)		
		0.004 M	0.02 M	0.04 M
CMC	Mean	100	100	100
	Std. Deviation	0	0	0
F20	Mean	33.83	79.28	92.63
	Std. Deviation	5.3	1.12	5.19
	CV (%)	15.67	1.41	5.60
Sig. probability		0	0	0.072
CMC	Mean	100	100	100
	Std. Deviation	0	0	0
F28	Mean	38	85.38	90.75
	Std. Deviation	18.99	2.49	1.8
	CV (%)	49.97	2.92	1.98
Sig. probability		0.006	0.001	0.001
CMC	Mean	100	100	100
	Std. Deviation	0	0	0
T1	Mean	51.19	57.12	87.4
	Std. Deviation	1.95	0.1	6.82
	CV (%)	3.81	0.18	7.80
Sig. probability		0	0	0.034

### 5.6. Nanoparticles formation in cellulose-silver suspensions

Cellulose-silver suspensions exhibited parasite phenomena due to silver nanoparticles (Ag-NPs) formation plus sedimentation. This phenomenon interferes with the correct measurements of silver solution standard peaks, therefore peaks around ~300 nm are higher than reference characteristic peaks. On the other hand, T1-silver suspensions displayed peaks attributed to the formation of these unstable Ag-NPs as shown in Figure 24. To be more specific, peaks around ~460 and ~490 nm appear in the spectra for different T1-copper suspensions, corresponding to the formation of unstable Ag-NPs (Nakamura et al., 2011).

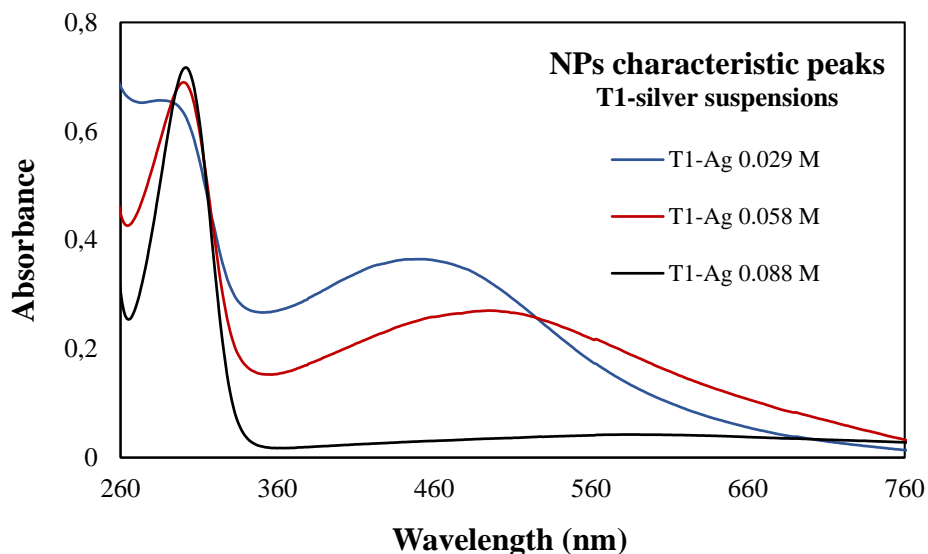


**Figure 24.** Absorption spectra of T1-silver suspensions

### 5.7. Samples surface properties

Surface analysis and volume pore data was only measured for control (CMC), F20, F25 and F28 cellulose samples, as illustrated in Table 11. Results showed that extracted cellulose samples present higher specific surface area and pore volumes compared to commercially available cellulose. To be more specific, F28 sample exhibit the largest specific surface area.

**Table 11.** Specific surface area (SSA) and pore volume (PV) of cellulose samples.

Sample	SSA (g/m <sup>2</sup> )	PV (m <sup>3</sup> /g)
CMC	3	0.018
F20	12	0.072
F25	9	0.061
F28	48	0.072

Moreover, in order to have a better understanding of the physicochemical properties that influence the adsorption capacities of cellulose samples, the correlation of specific surface area (SSA) and pore volume (PV) values is displayed in Figure 25.

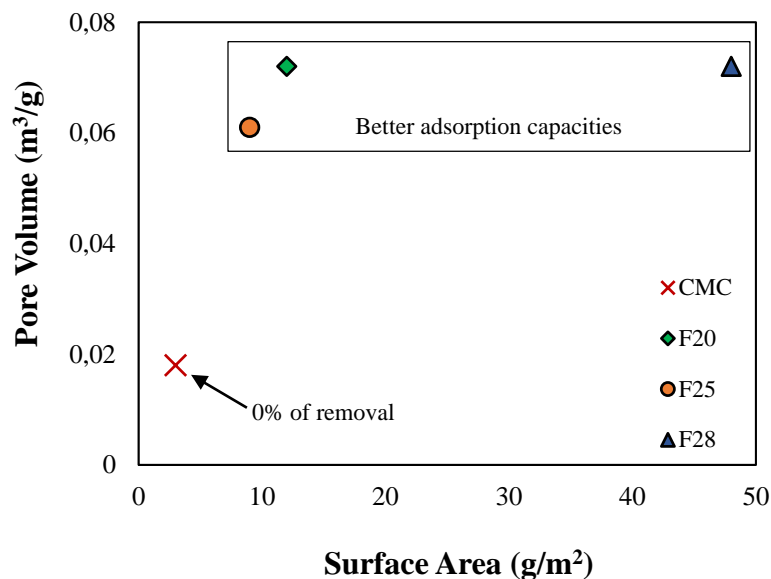


**Figure 25.** Correlation between PV and SSA

## 6. Discussion

Cellulose is a biopolymer available worldwide from a variety of biodiverse sources, which the literature has considered as a sustainable and environmental friendly biomaterial. Four different unmodified cellulose samples were successfully extracted from native natural sources of Ecuador. Seemingly, extracted cellulose samples present distinct and unique physico-chemical properties in comparison with the commercially available cellulose used as a control counterpart (CMC). Every sample was extracted following strictly the same protocol and characterized by using several techniques including FTIR, XRD, and SEM. Additional BET measurements were performed for three of the samples (F20, F25 and F28).

FTIR data of cellulose samples presented the same characteristic peaks of commercial cellulose control which demonstrates that F20, F25, F28 and T1 samples are mainly composed of cellulose and do not contain any other residual biopolymer such as hemicellulose and lignin. XRD diffraction showed the typical cellulose diffraction patterns and are similar to the control sample pattern. This fact indicates that the different crystallinity indexes depicted from cellulose samples may be attributed to the natural source from which they were extracted, since every sample was extracted and purified using the same procedure. CMC, the control sample, exhibited the highest crystalline index (78.1%) but did not reduce any heavy metal concentration. On the other hand, F20 (CrI: 28.2%), F25 (CrI: 36.8%) and

F28 (CrI: 56.2%) did reduce the concentration of copper (II) in aqueous solution. Thus, values of crystallinity appear to be a critical variable affecting the adsorption capacity of cellulose. However, in order to establish the suitable range of crystallinity degree in which cellulose presents the highest adsorption of copper cations, more experiments and analysis of other diverse cellulose samples should be conducted to have further information about ideal crystallinity degree. According to SEM observations, each cellulose sample presented unique morphology and structure differing in size, porosity and shapes. Therefore, the source is the main factor affecting the physico-chemical properties of the extracted cellulose.

Characteristic peaks of copper sulphate and silver nitrate solutions are similar to those presented in literature (Adadey & Sarfo, 2016; Aravinda et al. , 2012; Nakamura et al., 2011). Maximum absorbance values for each peak were collected to establish the calibration curves. Moreover, linear regression of calibration curves confirms that our tendency is totally linear and heavy metal concentrations can be readily measured using the linear equation with respect to the absorbance values of the solutions. Percentages of removal of cationic copper in cellulose-copper suspensions show that F20, F25, F28 and T1 samples adsorption capacities increase when the concentration of copper decreases. F20 fiber depicted the highest reduction percentage ( $66.17 \pm 5.3\%$ ) followed by F28 with a slightly lower percentage ( $62 \pm 18.99\%$ ) and T1 with the lowest ( $48.81 \pm 3.81\%$ ) when using 10 mg/mL cellulose concentration in 0.004 M solution. In contrast, statistical analysis suggests that T1 sample is the most effective cellulose particle for the removal of copper cations, since it presents the lowest coefficient of variances. On the other hand, when 1 mg/mL of cellulose concentration was applied, F28 sample emerged as the best adsorption agent ( $37.66 \pm 7.33\%$ ). In this case, statistical analysis supports that F28 sample will present the most efficient performance for removal of copper cations, since it exhibits a low coefficient of variance. Results suggest that adsorption capacities of cellulose particles are much better for lower copper concentrations and the ideal amount of cellulose should be above 10 mg in 1 mL solution. Indeed, HSD Tukey tests proved that the amount of cellulose is a significant effect factor that influences the adsorption capacities of cellulose particles, the higher the amount, the better the removal percentages. Additionally, it is important to highlight that cellulose samples were unmodified, therefore their adsorption capacities are directly attributable to their physicochemical features, such as the pore volume and the specific surface area. More



importantly, compared to functionalized cellulose-based materials described in literature (Rhaman et al., 2016; Setyono & Valiyaveetil, 2016), extracted cellulose particles presented in this research exhibits considerable adsorption capacities of copper cations, even though they were not modified. In contrast, the same cellulose samples did not show reliable results for silver nitrate solutions due to parasite phenomena (i.e. Ag-NPs formation plus sedimentation). Nonetheless, UV-Vis-NIR spectra of T1-silver suspensions depicted different peaks compared to the characteristic peaks of silver standard solutions, which is attributable to the formation of Ag-NPs, possibly due to the interaction between cellulose particles and silver nitrate molecules. Characteristic peaks of Ag-NPs are commonly reported in literature and values obtained in this research are identical (Nakamura et al., 2011; Rodríguez-león et al., 2013).

Sample surface characteristics were recorded in order to evaluate their influence on reduction capacities of cellulose samples (CMC, F20, F25 and F28). Figure 19 shows a correlation between pore volume and sample surface area from which it is clearly notable that cellulose particles exhibiting higher pore volumes are better for reduction of copper concentrations. On the other hand, sample surface areas demonstrated that this property is a crucial parameter for the adsorption capacity of cellulosic materials as F28 displayed the highest reduction percentage when using 1 mg/mL in 0.004 M copper sulphate solution. According to this data, the important factors to be considered to evaluate adsorption properties of cellulose-based materials are related to the surface and porosity degree.

## **7. Conclusion**

The present investigation is about untreated cellulose extracted from Ecuadorian natural sources as a possible solution to reduce the concentration levels of heavy metals present in water pollution, evaluating reduction capacities of cellulose samples. Unmodified cellulose isolates were successfully extracted and purified from different biodiverse sources of Ecuador, and called F20, F25, F28 and T1. Physicochemical characterization was performed on cellulose samples using FTIR, XRD, SEM and BET, and proved that every cellulose sample was obtained from different natural sources, which directly influences the physicochemical properties of the samples. Surface properties including sample surface area and pore volume are crucial factors affecting the heavy metal decontamination capabilities of the

samples. In fact, F28 and F20 samples exhibited the best performances in reduction capacities of copper concentration due to their surface area and pore volume parameters. However, F20 sample is more effective and reliable for cellulose-copper suspension with an initial concentration of 0.004 M, since it has a lower coefficient of variation. Seemingly, T1 sample presents low coefficient of variation as well as the best percentages of removal for higher concentrations of copper (II). Thereby, T1 emerges as the best cellulose particle for adsorption of copper cations due to its repeatability. Additionally, crystallinity degree might be considered as an important factor affecting decontamination properties of the cellulose samples.

The proposed hypothesis was partially demonstrated since all the results obtained from cellulose-silver suspensions were not precise due to the influence of parasite phenomena in heavy metal concentration. Indeed, the removal of silver in this case does not occur through an adsorption process; it happens via a reduction route that promotes the production of unstable Ag-NPs that sediment; this way, cationic silver is removed from the reaction mixture. However, further work, including deconvolution, is needed to thoroughly monitor this phenomenon. In spite of that, results data proved that T1 cellulose sample could be a potential agent for Ag-NPs formation. On the other hand, results obtained from cellulose-copper suspensions did show excellent results. Considering that MCL levels of heavy metals in drinking water are lower than the lowest concentration of Cu (II) used in this research, extracted cellulose samples emerged as good candidates for reduction of copper concentrations in aqueous solutions. Finally, this research clearly demonstrates the promising potential for exploring the biodiversity of Ecuador in order to create a wide range of unique cellulosic materials for environmental remediation.

## **8. Recommendations**

In order to have reliable and good UV-Vis-NIR measurements, it is recommended to centrifuge cellulose-treated samples at a speed higher than 5000 rpm for at least 5 min. After this, removing supernatant is imperative to avoid any possible cellulose particle when measuring the absorbance, because this can significantly interfere with UV-Vis-NIR measurement. Furthermore, atomic absorption spectroscopy may help in measuring very low

concentrations of heavy metals in aqueous solutions, and test solutions within the maximum contaminants levels.

It is also suggested to test cellulose samples for the removal of many other heavy metals present in polluted water. Thus, evaluating if cellulose can capture other heavy metal cations in aqueous solutions. Moreover, contaminated water samples containing many pollutants including a variety of heavy metals can be studied before and after treatment with cellulose particles. More importantly, the reusability of cellulose can be considered as a parameter for evaluation in future studies and the influence of permanence time of cellulose in polluted water solutions. As mentioned in the methodology, section 4.6, pellets were stored since elemental analysis can be carried out on samples.

## References

- Abiazem, C. V., Williams, A. B., Inegbenebor, I. A., Onwordi, C. T., Ehi-Eromosele, C. O., & Petrik, L. F. (2019). Adsorption of lead ion from aqueous solution onto cellulose nanocrystal from cassava peel. *International Conference on Science and Sustainable Development*. <https://doi.org/10.1088/1742-6596/1299/1/012122>
- Adadey, S. M., & Sarfo, J. K. (2016). Copper-paracetamol complexes : Promising lead antibacterial drug candidates. *African Journal of Pure and Applied Chemistry*, *10*(5), 56–62. <https://doi.org/10.5897/AJPAC2016.0701>
- Ahmad, S., Pandey, A., & Pathak, V. V. (2020). Phycoremediation : Algae as Eco-friendly Tools for the Removal of Heavy Metals from Wastewaters. *Bioremediation of Industrial Waste for Environmental Safety*, 53–76. [https://doi.org/10.1007/978-981-13-3426-9\\_3](https://doi.org/10.1007/978-981-13-3426-9_3)
- Alawam, K. (2014). Application of Proteomics in Diagnosis of ADHD , Schizophrenia , Major Depression , and Suicidal Behavior. In *Proteomics in Biomedicine and Pharmacology* (1st ed., Vol. 95). <https://doi.org/10.1016/B978-0-12-800453-1.00009-9>
- Anwar, B., Bundjali, B., & Arcana, I. M. (2015). Isolation of Cellulose Nanocrystals from Bacterial Cellulose Produced from Pineapple Peel Waste Juice as Culture Medium. *Procedia Chemistry*, *16*, 279–284. <https://doi.org/10.1016/j.proche.2015.12.051>
- Aravinda, C., Mayanna, S., & Muralidharan, V. (2012). Electrochemical behaviour of alkaline copper complexes. *Journal of Chemical Sciences*, *112*(5), 543–550. <https://doi.org/10.1007/BF02709287>
- Auta, R., Adamus, G., Kwiecien, M., Radecka, I., & Hooley, P. (2017). Production and characterization of bacterial cellulose before and after enzymatic hydrolysis. *African Journal of Biotechnology*, *16*(10), 470–482. <https://doi.org/10.5897/AJB2016.15486>
- Banco de Desarrollo del Ecuador. (2017). Programa Agua y Saneamiento para Todos. Retrieved from BDE web page website: <https://bde.fin.ec/project/programa-agua-y-saneamiento-para-todos/>
- Barakat, M. A. (2011). *New trends in removing heavy metals from industrial wastewater*. 361–377. <https://doi.org/10.1016/j.arabjc.2010.07.019>
- Bethke, K., Palantöken, S., Andrei, V., Roß, M., Raghuvanshi, V. S., Kettemann, F., ... Rademann, K. (2018). Functionalized Cellulose for Water Purification, Antimicrobial Applications, and Sensors. *Advanced Functional Materials*, *28*(23), 1–14. <https://doi.org/10.1002/adfm.201800409>
- Bissen, M., Frimmel, F. H., & Ag, C. (2003). Arsenic – a Review. Part I: Occurrence , Toxicity , Speciation , Mobility. *Acta Hydrochimica et Hydrobiologica*, *31*(1), 9–18.
- Brigham, C. (2018). Biopolymers : Biodegradable Alternatives to Traditional Plastics. In *Green Chemistry*. <https://doi.org/10.1016/B978-0-12-809270-5.00027-3>
- Carpenter, A. W., De Lannoy, C. F., & Wiesner, M. R. (2015). Cellulose nanomaterials in water treatment technologies. *Environmental Science and Technology*, *49*(9), 5277–5287. <https://doi.org/10.1021/es506351r>
- Costa, L. A. S., Assis, D. D. J., Gomes, G. V. P., Jania, B. A., Fonsêca, A. F., & Druzian, J. I. (2015). Extraction and characterization of nanocellulose from corn stover. *Materials Today: Proceedings*, *2*(1), 287–294. <https://doi.org/10.1016/j.matpr.2015.04.045>
- Dai, X., Song, H., Liu, W., & Wang, G. (2016). On-line UV-NIR spectroscopy as a process analytical technology (PAT) tool for on-line and real-time monitoring of the extraction process of Coptis Rhizome. *RSC Advances*, *6*, 10078–10085. <https://doi.org/10.1039/C5RA23688F>
- Day, Z. B. (2016). Preliminary Studies in Using X-Ray Diffraction for Analyzing the Atomic Structure of Central Plains Tradition Constituents. *Anthropology Department Theses and Dissertations*.

- Dhyani, V., & Bhaskar, T. (2019). Pyrolysis of Biomass. In *Biofuels: Alternative Feedstocks and Conversion Processes for the Production of Liquid and Gaseous Biofuels (Second Edition)* (pp. 217–244). <https://doi.org/10.1016/B978-0-12-816856-1.00009-9>
- Duruibe, J., Ogwuegbu, M., & Egwurugwu, J. (2007). Heavy metal pollution and human biotoxic effects. *International Journal of Physical Sciences*, 2(5), 112–118.
- Dwivedi, C., Pandey, I., Pandey, H., Ramteke, P. W., Pandey, A. C., Bhushan, S., & Patil, S. (2017). Electrospun Nanofibrous Scaffold as a Potential Carrier of Antimicrobial Therapeutics for Diabetic Wound Healing and Tissue Regeneration. In *Nano- and Microscale Drug Delivery Systems*. <https://doi.org/10.1016/B978-0-323-52727-9/00009-1>
- Enr, P., Pesantes, A. A., Carpio, E. P., Vitvar, T., Mar, M., Mahamud, L., ... Niño, E. (2019). *A Multi-Index Analysis Approach to Heavy Metal Pollution Assessment in River Sediments in the*. <https://doi.org/10.3390/w11030590>
- George, J., & Sabapathi, S. (2015). Cellulose nanocrystals : synthesis , functional properties , and applications. *Nanotechnology, Sciences and Applications*, 45–54.
- González, V., Valle, S., Nirchio, M., Olivero, J., Tejada, L., Valdelamar, J., ... González, K. (2018). Evaluación del riesgo de contaminación por metales pesados (Hg y Pb) en sedimentos marinos del Estero Huaylá, Puerto Bolívar, Ecuador. *Revista Del Instituto De Investigación De La Facultad De Ingeniería Geológica, Minera, Metalúrgica Y Geográfica*, 21(41), 75–82.
- Guclu, G., Gurdag, G., & Ozgumus, S. (2003). Competitive Removal of Heavy Metal Ions by Cellulose Graft Copolymers. *Journal of Applied Polymer Science*, 90(8), 2034–2039.
- Guerra, F. D., Campbell, M. L., Attia, M. F., Whitehead, D. C., & Alexis, F. (2018). Capture of Aldehyde VOCs Using a Series of Amine-Functionalized Cellulose Nanocrystals. *ChemistrySelect*, 3(20), 5495–5501. <https://doi.org/10.1002/slct.201703149>
- Harari, R., & Harari, H. (2006). Children’s Environment and Health in Latin America: The Ecuadorian Case. *Annals of the New York Academy of Sciences*, 1076(1), 660–677. <https://doi.org/10.1196/annals.1371.082>
- Instituto Ecuatoriano de Normalización (INEN). *Norma técnica ecuatoriana. Agua Potable. Requisitos.* , (2014).
- Inyinbor Adejumo, A., Adebisin Babatunde, O., Abimbola, O., Tabitha, A., P, O. A., & A, A. T. (2018). Water Pollution : Effects , Prevention , and Climatic Impact, Water Challenges of an Urbanizing World,. *IntechOpen*. <https://doi.org/10.5772/intechopen.72018>
- Jaishankar, M., Tseten, T., Anbalagan, N., Mathew, B. B., & Beeregowda, K. N. (2014). Toxicity, mechanism and health effects of some heavy metals. *Interdisciplinary Toxicology*, 7(2), 60–72. <https://doi.org/10.2478/intox-2014-0009>
- Lavanya, D., Kulkarni, P., & Dixit, M. (2011). Sources of cellulose and their applications- A review. *International Journal of Drug Formulation and Research*, 2(6).
- Lee, L. Z., Abbas, M., Zaini, A., & Tang, S. H. (2019). Porous Nanomaterials for Heavy Metal Removal 20. *Handbook of Ecomaterials*, 469–494. [https://doi.org/10.1007/978-3-319-68255-6\\_27](https://doi.org/10.1007/978-3-319-68255-6_27)
- Ma, H., Burger, C., Hsiao, B. S., & Chu, B. (2011). Ultra-fine cellulose nanofibers: New nano-scale materials for water purification. *Journal of Materials Chemistry*, 21(21), 7507–7510. <https://doi.org/10.1039/c0jm04308g>
- McClintock, T. R., Chen, Y., Bundschuh, J., Oliver, J. T., Navoni, J., Olmos, V., ... Parvez, F. (2012). Arsenic Exposure in Latin America: Biomarkers, Risk Assessments and Related Health Effects. *The Science of the Total Environment*, 429, 76–91. <https://doi.org/10.1016/j.scitotenv.2011.08.051>. Arsenic
- Mihiranyan, A. (2010). Cellulose from cladophorales green algae: From environmental problem to high-tech

- composite materials. *Journal of Applied Polymer Science*, 119(4), 2449–2460.  
<https://doi.org/10.1002/app>
- Morán, J. I., Alvarez, V. A., Cyras, V. P., & Vázquez, A. (2008). Extraction of cellulose and preparation of nanocellulose from sisal fibers. *Cellulose*, 15(1), 149–159. <https://doi.org/10.1007/s10570-007-9145-9>
- Nabili, A., Fattoum, A., Passas, R., Elaloui, E., & Nabili, A. (2014). Extraction and characterization of cellulose from date palm seeds (*Phoenix dactylifera* L.). *Cellulose Chemistry and Technology*, 50, 9–10.
- Nakamura, T., Magara, H., Herbani, Y., & Sato, S. (2011). Fabrication of silver nanoparticles by highly intense laser irradiation of aqueous solution. *Applied Physics*, 1021–1024.  
<https://doi.org/10.1007/s00339-011-6499-5>
- O’Connell, D. W., Birkinshaw, C., & O’Dwyer, T. F. (2008). Heavy metal adsorbents prepared from the modification of cellulose: A review. *Bioresource Technology*, 99(15), 6709–6724.  
<https://doi.org/10.1016/j.biortech.2008.01.036>
- Oviedo-Anchundia, R., Moina-quimí, E., Naranjo-morán, J., & Barcos-arias, M. (2017). Contaminación por metales pesados en el sur del Ecuador asociada a la actividad minera . Contamination by heavy metals in the south of Ecuador associated to the mining activity . *Bionatura*.
- Phanthong, P., Reubroycharoen, P., Hao, X., Xu, G., Abudula, A., & Guan, G. (2018). Nanocellulose : Extraction and application. *Carbon Resources Conversion*, 1(1), 32–43.  
<https://doi.org/10.1016/j.crcon.2018.05.004>
- Ramírez, L., Mátyás, B., & Lozano-Haro, Z. J. (2019). Modelling risk using Bayes theorem of infection by antibiotic-resistant *Escherichia coli* in rural and urban populations of Ecuador [version 1; peer review: 2 approved, 1 approved with reservations]. *FI000Research*, 7, 375.
- Rebolledo, E., & Jiménez, P. (2012). Afectaciones a la calidad de agua en el norte de la provincia de Esmeraldas producto de la minería aurífera ilegal en el año 2011. *Primer Seminario Científico Internacional Medioambiente Economía y Desarrollo*. <https://doi.org/10.13140/2.1.4153.0563>
- Rhaman, M. L., Sarkar, S. M., Yusoff, M. M., Kulkarni, A. K. D., Chowdhury, Z. Z., & Ali, M. E. (2016). Poly(amidoxime) from Polymer-Grafted Khaya Cellulose: An Excellent Medium for the Removal of Transition Metal Cations from Aqueous Solution. *BioResources*, 11(3), 6780–6800.
- Rodríguez-león, E., Iñiguez-palomares, R., Navarro, R. E., Herrera-urbina, R., & Tánori, J. (2013). Synthesis of silver nanoparticles using reducing agents obtained from natural sources ( *Rumex hymenosepalus* extracts ). *Nanoscale Research Letters*, 8(1), 1–10. <https://doi.org/10.1186/1556-276X-8-318>
- Roncero Vivero, M. (2000). *Obtención de una secuencia TFC con la aplicación de ozono y enzimas, para el blanqueo de pastas madereras y de origen agrícola. Optimización de la etapa Z. Análisis de los efectos en la fibra celulósica y sus componentes*. Universidad Politécnica de Cataluña.
- Segal, L., Creely, J. J., Martin, A. E., & Conrad, C. M. (1959). An Empirical Method for Estimating the Degree of Crystallinity of Native Cellulose Using the X-Ray Diffractometer. *Textile Research Journal*, 29(10), 786–794. <https://doi.org/10.1177/004051755902901003>
- Setyono, D., & Valiyaveetil, S. (2016). Functionalized paper - A readily accessible adsorbent for removal of dissolved heavy metal salts and nanoparticles from water. *Journal of Hazardous Materials*, 302, 120–128. <https://doi.org/10.1016/j.jhazmat.2015.09.046>
- Swinehart, D. (1962). Beer-Lambert Law. *Journal of Chemical Education*, 39(7), 333–335.  
<https://doi.org/10.1021/ed039p333>
- Tarras-wahlberg, N. H., Flachier, A., Lane, S. N., & Sangfors, O. (2001). Environmental impacts and metal exposure of aquatic ecosystems in rivers contaminated by small scale gold mining : the Puyango River basin , southern Ecuador. *Science of the Total Environment*, 278(1–3), 239–261.
- Tchounwou, P. B., Yedjou, C. G., Patlolla, A. K., & Sutton, D. J. (2012). Heavy Metal Toxicity and the

- Environment. *Experientia Supplementum*, 101, 133–164. <https://doi.org/10.1007/978-3-7643-8340-4>
- Thakur, V. K., & Thakur, M. K. (2014). Processing and characterization of natural cellulose fibers/thermoset polymer composites. *Carbohydrate Polymers*, Vol. 109, pp. 102–117. <https://doi.org/10.1016/j.carbpol.2014.03.039>
- Tian, Y., Wu, M., Liu, R., Li, Y., Wang, D., Tan, J., ... Huang, Y. (2011). Electrospun membrane of cellulose acetate for heavy metal ion adsorption in water treatment. *Carbohydrate Polymers*, 83(2), 743–748. <https://doi.org/10.1016/j.carbpol.2010.08.054>
- Tursi, A., Beneduci, A., Chidichimo, F., Vietro, N. De, & Chidichimo, G. (2018). Remediation of hydrocarbons polluted water by hydrophobic functionalized cellulose. *Chemosphere*, (201), 530–539. <https://doi.org/10.1016/j.chemosphere.2018.03.044>
- Unemi, R. C. (2016). Calidad del agua destinada al consumo humano en un cantón de Ecuador Quality of water intended for human consumption in a canton of Ecuador. *Revista Ciencia UNEMI*, 9, 109–117.
- Varghese, A. G., Annie, S., & Latha, P. M. S. (2018). Remediation of heavy metals and dyes from wastewater using cellulose-based adsorbents. *Environmental Chemistry Letters*. <https://doi.org/10.1007/s10311-018-00843-z>
- Velásquez, P. C., Veiga, M. M., & Hall, K. (2010). Mercury balance in amalgamation in artisanal and small-scale gold mining: identifying strategies for reducing environmental pollution in Portovelo-Zaruma, Ecuador. *Journal of Cleaner Production*, 18(3), 226–232. <https://doi.org/10.1016/j.jclepro.2009.10.010>
- Verma, R., & Dwivedi, P. (2013). Heavy metal water pollution- A case study. *Recent Research in Science and Technology*, 5(5), 98–99.
- Waly, A., Aly, A. S., & Hebeish, A. (1998). Synthesis and Characterization of Cellulose Ion Exchanger . II . Pilot Scale and Utilization in Dye – Heavy Metal Removal. *Journal of Applied Polymer Science*, 68(13), 2151–2157.
- Wan Ngah, W. S., & Hanafiah, M. A. K. M. (2008). Removal of heavy metal ions from wastewater by chemically modified plant wastes as adsorbents: A review. *Bioresource Technology*, 99(10), 3935–3948. <https://doi.org/10.1016/j.biortech.2007.06.011>
- Wang, S., Sun, H., Ang, H. M., & Tadé, M. O. (2013). Adsorptive remediation of environmental pollutants using novel graphene-based nanomaterials. *Chemical Engineering Journal*. <https://doi.org/10.1016/j.cej.2013.04.070>
- Wang, Y., Wang, X., Xie, Y., & Zhang, K. (2018). Functional nanomaterials through esterification of cellulose : a review of chemistry and application. *Cellulose*, 25(7), 3703–3731. <https://doi.org/10.1007/s10570-018-1830-3>
- World Health Organization. (2001). *Water for health: Taking charge*.
- World Health Organization. (2011). *Adverse Health Effects of Heavy Metals in Children*.
- Zhou, W., Apkarian, R. P., & Wang, Z. L. (2006). Fundamentals of Scanning Electron Microscopy. In *Scanning Microscopy for Nanotechnology* (pp. 1–40). [https://doi.org/10.1007/978-0-387-39620-0\\_1](https://doi.org/10.1007/978-0-387-39620-0_1)

## Annex A

Table 12. Maximum values of absorbance of cellulose-copper suspensions

Maximum values of absorbance				
Cellulose Sample		Concentrations of copper solutions		
		0.004 M	0.02 M	0.04 M
CMC	1 mg/mL	0.0531	0.2558	0.5022
		0.0524	0.2556	0.5029
		0.0527	0.2561	0.503
	10 mg/mL	0.0601	0.2543	0.5022
		0.0513	0.256	0.5008
		0.0518	0.2559	0.5032
F20	1 mg/mL	0.0453	0.2434	0.4917
		0.0525	0.2365	0.4828
		0.0478	0.2426	0.4676
	10 mg/mL	0.0175	0.201	0.4362
		0.0206	0.2005	0.4858
		0.0151	0.2057	0.475
F28	1 mg/mL	0.0362	0.2435	0.4667
		0.0286	0.2345	0.4821
		0.0329	0.2252	0.4634
	10 mg/mL	0.0106	0.2107	0.4454
		0.0245	0.2214	0.4614
		0.0297	0.222	0.4606
F25	1 mg/mL	0.052	0.2328	0.5083
		0.0265	0.2191	0.4902
		0.0384	0.2325	0.4857
T1	10 mg/mL	0.0261	0.1461	0.4505
		0.0278	0.1456	0.4675
		0.026	0.1458	0.4015



**Table 13. Copper remaining percentages in cellulose-copper suspensions**

Copper remaining percentages (%)				
Cellulose Sample		Concentrations		
		0.004 M	0.02 M	0.04 M
CMC	1 mg/mL	100	100	100
		100	100	100
		100	100	100
	10 mg/mL	100	100	100
		100	100	100
		100	100	100
F20	1 mg/mL	87.12	95.34	97.91
		100	92.64	96.14
		91.92	95.03	93.11
	10 mg/mL	33.65	78.73	86.86
		39.62	78.54	96.73
		29.04	80.57	94.58
F28	1 mg/mL	69.62	95.38	92.93
		55	91.85	96
		63.27	88.21	92.27
	10 mg/mL	20.38	82.53	88.69
		47.12	86.72	91.88
		57.12	86.96	91.72
F25	1 mg/mL	100	91.19	100
		50.96	85.82	97.61
		73.85	91.07	96.71
T1	10 mg/mL	50.19	57.23	89.71
		53.46	57.03	93.09
		50	57.11	79.95

**Table 14. Values of absolute concentration in cellulose-copper suspensions**

Values of Absolute Concentration				
Cellulose Sample		Concentrations of copper solutions		
Treatment	Amount	0.004 M	0.02 M	0.04 M
CMC	1 mg/mL	0.00408462	0.02004702	0.04
		0.00403077	0.02003135	0.04005575
		0.00405385	0.02007053	0.04006372
	10 mg/mL	0.00462308	0.01992947	0.04
		0.00394615	0.0200627	0.03988849
		0.00398462	0.02005486	0.04007965
F20	1 mg/mL	0.00348462	0.01907524	0.03916368
		0.00403846	0.01853448	0.0384548
		0.00367692	0.01901254	0.03724413
	10 mg/mL	0.00134615	0.01575235	0.03474313
		0.00158462	0.01571317	0.03869375
		0.00116154	0.01612069	0.03783353
F28	1 mg/mL	0.00278462	0.01908307	0.03717244
		0.0022	0.01837774	0.03839904
		0.00253077	0.0176489	0.0369096
	10 mg/mL	0.00081538	0.01651254	0.03547591
		0.00188462	0.0173511	0.0367503
		0.00228462	0.01739812	0.03668658
F25	1 mg/mL	0.004	0.01824451	0.04048586
		0.00203846	0.01717085	0.03904421
		0.00295385	0.018221	0.03868578
T1	10 mg/mL	0.00200769	0.01144984	0.03588212
		0.00213846	0.01141066	0.03723616
		0.002	0.01142633	0.03197929

## Annex B

## Raw data of HSD Tukey tests

HSD Tukey of effect factor "Cellulose sample" for copper-cellulose suspensions (0.004 M)						
Cellulose sample	Means	Std	r	Min	Max	Groups
CMC	0.004121	2.51E-04	6	0.003946	0.004623	a
F20	0.002549	1.32E-03	6	0.001162	0.004038	b
F25	0.002997	9.81E-04	3	0.002038	0.004000	b
F28	0.002083	6.92E-04	6	0.000815	0.002785	b
T1	0.002049	7.78E-05	3	0.002000	0.002138	b

HSD Tukey of effect factor "Amount of cellulose" for copper-cellulose suspensions (0.004 M)						
Amount of cellulose	Means	Std	r	Min	Max	Groups
1 mg/mL	0.003323	7.81E-04	12	0.002038	0.004085	a
10 mg/mL	0.002315	1.21E-03	12	0.000815	0.004623	b

HSD Tukey of effect factor "Cellulose sample" for copper-cellulose suspensions (0.02 M)						
Cellulose sample	Means	Std	r	Min	Max	Groups
CMC	0.020033	5.23E-05	6	0.019929	0.020071	a
F20	0.017368	1.67E-03	6	0.015713	0.019075	b
F25	0.017879	6.13E-04	3	0.017171	0.018245	b
F28	0.017729	8.94E-04	6	0.016513	0.019083	b
T1	0.011429	1.97E-05	3	0.011411	0.011450	c

HSD Tukey of effect factor "Amount of cellulose" for copper-cellulose suspensions (0.02 M)						
Amount of cellulose	Means	Std	r	Min	Max	Groups
1 mg/mL	0.018793	9.42E-04	12	0.017171	0.020071	a
10 mg/mL	0.016098	3.24E-03	12	0.011411	0.020063	b

HSD Tukey of effect factor "Cellulose sample" for copper-cellulose suspensions (0.04 M)						
Cellulose sample	Means	Std	r	Min	Max	Groups
CMC	0.040015	7.02E-05	6	0.039888	0.040080	a
F20	0.037689	1.59E-03	6	0.034743	0.039164	abc
F25	0.039405	9.53E-04	3	0.038686	0.040486	ab
F28	0.036899	9.40E-04	6	0.035476	0.038399	bc
T1	0.035033	2.73E-03	3	0.031979	0.037236	c

<b>HSD Tukey of effect factor "Amount of cellulose" for copper-cellulose suspensions (0.04 M)</b>						
Amount of cellulose	Means	Std	r	Min	Max	Groups
1 mg/mL	0.038807	1.23E-03	12	0.036910	0.040486	a
10 mg/mL	0.037104	2.42E-03	12	0.031979	0.040080	b